



UWS Academic Portal

U-Pb zircon age dating of diamond-bearing gneiss from Fjørtoft reveals repeated burial of the Baltoscandian margin during the Caledonian Orogen

Walczak, Katarzyna; Cuthbert, Simon; Kooijman, Ellen Kooijman; Majka, Jaroslav; Smit, Matthias

Published in:
Geological Magazine

DOI:
[10.1017/S0016756819000268](https://doi.org/10.1017/S0016756819000268)

Published: 30/11/2019

Document Version
Peer reviewed version

[Link to publication on the UWS Academic Portal](#)

Citation for published version (APA):

Walczak, K., Cuthbert, S., Kooijman, E. K., Majka, J., & Smit, M. (2019). U-Pb zircon age dating of diamond-bearing gneiss from Fjørtoft reveals repeated burial of the Baltoscandian margin during the Caledonian Orogen. *Geological Magazine*, 156(11), 1949-1964. [GEO-18-2102.R2]. <https://doi.org/10.1017/S0016756819000268>

General rights

Copyright and moral rights for the publications made accessible in the UWS Academic Portal are retained by the authors and/or other copyright owners and it is a condition of accessing publications that users recognise and abide by the legal requirements associated with these rights.

Take down policy

If you believe that this document breaches copyright please contact pure@uws.ac.uk providing details, and we will remove access to the work immediately and investigate your claim.

**U-Pb zircon age dating of diamond-bearing gneiss from
Fjørtoft reveals repeated burial of the Baltoscandian margin
during the Caledonian Orogeny**

Journal:	<i>Geological Magazine</i>
Manuscript ID	GEO-18-2102.R2
Manuscript Type:	Original Article
Date Submitted by the Author:	19-Feb-2019
Complete List of Authors:	Walczak, Katarzyna; AGH University of Science and Technology , Faculty of Geology, Geophysics and Environmental Protection Cuthbert, Simon; School of Computing, Engineering & Physical Sciences, University of the West of Scotland, Paisley, United Kingdom Kooijman, Ellen; Swedish Museum of Natural History, Department of Geosciences Majka, Jaroslaw; Uppsala University, Department of Earth Sciences; AGH University of Science and Technology , Faculty of Geology, Geophysics and Environmental Protection Smit, Matthijs; University of British Columbia, Department of Earth, Ocean and Atmospheric Sciences
Keywords:	geochronology, Western Gneiss Region, ultrahigh pressure metamorphism, U-Pb zircon dating

1
2
3
4
5
6
7
8
9
10
11
12
13
14
15
16
17
18
19
20
21
22
23
24
25
26
27
28
29
30
31
32
33
34
35
36
37
38
39
40
41
42
43
44
45
46
47
48
49
50
51
52
53
54
55
56
57
58
59
60

U-Pb zircon age dating of diamond-bearing gneiss from Fjortoft reveals repeated burial of the Baltoscandian margin during the Caledonian Orogeny

Katarzyna Walczak¹, Simon Cuthbert², Ellen Kooijman³, Jarosław Majka^{1,4}, Matthijs A. Smit⁵

¹ Faculty of Geology, Geophysics and Environmental Protection, AGH University of Science and Technology, Kraków, Poland

² School of Computing, Engineering & Physical Sciences, University of the West of Scotland, Paisley, United Kingdom

³ Department of Geosciences, Swedish Museum of Natural History, Stockholm, Sweden

⁴ Department of Earth Sciences, Uppsala University, Villavägen 16 SE-752 36 Uppsala, Sweden

⁵ Department of Earth, Ocean and Atmospheric Sciences, University of British Columbia, Vancouver, British Columbia, Canada

Corresponding author:
Katarzyna Walczak, Faculty of Geology, Geophysics and Environmental Protection,
AGH University of Science and Technology, Mickiewicza 30, 30-059 Kraków, Poland
Email: kwalczak@agh.edu.pl

Short title:
U-Pb zircon dating of diamondiferous gneiss, WGR

24 **ABSTRACT**

25 The first find of micro-diamond in the Nordøyane UHP domain of the Western Gneiss
26 Region (WGR) of the Scandinavian Caledonides reshaped tectonic models for the region.
27 Nevertheless, in spite of much progress regarding the meaning and significance of this
28 find, the history of rock that the diamonds were found in is complex and still largely
29 ambiguous. To investigate this, we report U-Pb zircon ages obtained from the exact
30 crushed sample material in which metamorphic diamond was first found. The grains
31 exhibit complicated internal zoning with distinct detrital cores overgrown by
32 metamorphic rims. The cores yielded a range of ages from the Archean to the late
33 Neoproterozoic/early Cambrian. This detrital zircon age spectrum is broadly similar to
34 detrital signatures recorded by metasedimentary rocks of the Lower and Middle
35 allochthons elsewhere within the orogen. Thus, our dating results support the previously
36 proposed affinity of the studied gneiss to the Seve-Blåhø Nappe of the Middle
37 Allochthon. Metamorphic rims yielded a well-defined peak at 447 ± 2 Ma and a broad
38 population that ranges between *c.* 437 and 423 Ma. The data reveal a prolonged
39 metamorphic history of the Fjærtøft gneiss that is far more complex than would be
40 expected for an UHP rock that has seen a single burial and exhumation cycle. The data
41 are consistent with a model involving multiple such cycles, which would provide
42 renewed support for the tectonics model that has been postulated for the region.

44 Key words: geochronology, Western Gneiss Region, ultrahigh pressure metamorphism

46 **1. Introduction**

1
2
3
4
5
6
7
8
9
10
11
12
13
14
15
16
17
18
19
20
21
22
23
24
25
26
27
28
29
30
31
32
33
34
35
36
37
38
39
40
41
42
43
44
45
46
47
48
49
50
51
52
53
54
55
56
57
58
59
60

The Scandinavian Caledonides is an archetypal collisional orogen, containing some of the world's best preserved and most spectacular examples of deeply buried continental rocks. The mountain belt formed between the late Cambrian (Furongian) to early Ordovician and the late Silurian to early Devonian (e.g. Gee *et al.* 2013 and references therein), when the Iapetus basin contracted towards closure and multiple subduction-collision events occurred between the hyper-extended margin of Baltica and the outboard terranes (island arcs and/or microcontinents). The terminus of this period was the collision between Baltica and Laurentia, with the former undergoing transient subduction deeply beneath the latter (e.g. Krogh, 1977; Andersen *et al.* 1991; Brueckner & van Roermund, 2004; Majka *et al.* 2014). The various subduction-collision processes produced a multitude of (ultra-)high pressure (UHP-HP) rock types yielding various ages of peak metamorphism. The most pronounced of the early (late Cambrian and early to mid-Ordovician) UHP-HP events are those recorded in the Middle Allochthon (*sensu* e.g. Gee *et al.* 2010), which is exposed along the entire length of the Scandinavian Caledonides. UHP rocks are currently known from several localities spanning almost the full length of the outcrop of the Middle Allochthon, a few of which contain well-established metamorphic microdiamond (e.g. Smit *et al.* 2010; Janák *et al.* 2013; Majka *et al.* 2014; Gillio *et al.* 2015; Klonowska *et al.* 2016, 2017; Bukala *et al.* 2018). While these occurrences are widely spaced and UHP metamorphism may not have been continuous or exactly contemporaneous between them, subduction of the Baltica continental margin was clearly an important and widespread process during the Caledonian orogenic cycle prior to the final Scandian collision.

1
2
3 69 Vestiges of the Middle Allochthon also occur as deep infolds or tectonic intercalations
4
5 70 within the largest UHP-HP province in the Scandinavian Caledonides (Terry &
6
7 71 Robinson, 2004; Robinson *et al.* 2014), the Western Gneiss Region (WGR), which is a
8
9
10 72 large tectonic window in which the Baltic cratonic margin, intensively reworked,
11
12 73 emerges in the hinterland through the pile of allochthons. This giant UHP terrane
13
14 74 represents the deeply subducted margin of Baltica (Krogh, 1977; Cuthbert *et al.* 1983).
15
16
17 75 Here, the Middle Allochthon is intimately associated with HP or UHP Baltica basement
18
19 76 rocks (Terry & Robinson, 2004). Differences between the ages for UHP metamorphism
20
21 77 in the Middle Allochthon in Sweden (Ordovician) and in the basement orthogneisses of
22
23 78 the WGR (latest Silurian to early Devonian) suggest that inliers of the Middle Allochthon
24
25 79 in the WGR could have undergone both Ordovician and Silurian-Devonian
26
27 80 metamorphism and thus may have been subducted at least twice during the Caledonian
28
29
30
31 81 orogenic cycle.
32
33 82 The possibility of dual or even multiple subduction episodes was embodied in the ‘dunk
34
35 83 tectonics’ evolutionary model proposed by Brueckner & van Roermund (2004) and
36
37 84 Brueckner (2006) and revived by Majka *et al.* (2014), in which a continental margin is
38
39 85 repeatedly subducted into the mantle (‘dunked’) during successive collisions with arcs
40
41 86 and continental fragments during ocean closure, including the climactic final continental
42
43
44 87 collision. The dunk tectonics model predicts repeated UHP-HP metamorphism across
45
46 88 laterally extensive domains of the terranes now dispersed among the thrust stack in the
47
48 89 orogenic foreland. If this is the case, the early to mid-Ordovician subduction-related
49
50 90 metamorphism recorded in the Seve nappes exposed in Sweden (e.g. Janák *et al.* 2013;
51
52
53 91 Klonowska *et al.* 2017; Bukala *et al.* 2018) should also have affected the Blåhø Nappe
54
55
56
57
58
59
60

1
2
3
4
5
6
7
8
9
10
11
12
13
14
15
16
17
18
19
20
21
22
23
24
25
26
27
28
29
30
31
32
33
34
35
36
37
38
39
40
41
42
43
44
45
46
47
48
49
50
51
52
53
54
55
56
57
58
59
60

(Middle Allochthon) in the WGR, but would have been strongly overprinted by the late Silurian-Devonian ‘Scandian’ collision between Baltica and Laurentia and the resulting (U)HP metamorphism that is so spectacularly recorded in the WGR basement. Tracing this early subduction record into the highest-grade domains of the WGR deep within the orogenic core has, indeed, proved difficult thus far. (U)HP rocks in these domains mostly belong to the Baltic basement and record only Siluro-Devonian (Scandian; 425-400 Ma) overprinting. However, a well-known but enigmatic occurrence of high-grade pelitic gneiss outcropping in the Nordøyane area of western Norway has yielded microdiamond (Dobrzhinetskaya *et al.* 1995) and thus shows petrological similarity to some metapelitic UHP rocks in the Seve Nappe Complex near the Caledonide foreland (Klonowska *et al.* 2017). To trace the history of high-grade allochthonous rocks in the WGR and ultimately test the efficacy of the dunk tectonics model, we subjected zircon from this unusual lithology to U-Pb zircon chronology. These rocks have long been ascribed to the Seve-Blåhø Nappe of the Middle Allochthon (e.g. Krill, 1985) and thus may provide a record of earlier metamorphic cycles that are otherwise overlooked or lacking.

2. Geological setting

This study focuses on high-grade gneisses exposed within the northern part of the WGR (Fig. 1a) - a giant Baltic (U)HP terrane exposed in the high-grade core of the Scandinavian Caledonides of western Norway (e.g. Hacker *et al.* 2010, 2015). The WGR is predominantly composed of felsic-to-intermediate orthogneisses and psammitic metasediments with Mesoproterozoic and Neoproterozoic protoliths derived from the Fennoscandian craton and its pre- to syn-orogenic metasedimentary cover (the ‘para-

1
2
3 115 autochthon') rocks (e.g. Krill, 1980, 1985; Gaal & Gorbatshev, 1987; Tucker *et al.*
4
5 116 1991, 2004; Robinson *et al.* 2014; Young, 2018). Near the southeastern margin of the
6
7
8 117 WGR, the terrane is dominated by rocks resembling the pristine Baltican basement rocks
9
10 118 of the foreland. Towards the northwest and west, however, the basement rocks are
11
12 119 intensely *Caledonized*, i.e. reworked by Caledonian tectonism and metamorphism, and
13
14
15 120 show widespread evidence for (U)HP metamorphism, mainly in the form of abundant
16
17 121 pods of eclogite, but also HP or UHP felsic rocks (Krogh, 1977; Griffin & Brueckner,
18
19 122 1985; Cuthbert *et al.* 2000; Hacker *et al.* 2010). In the highest-P parts of the WGR
20
21 123 several isolated bodies of mantle-derived ultramafic rocks including dunite, garnet
22
23 124 peridotite and garnet pyroxenites appear (e.g. Brueckner *et al.* 2010), reinforcing the
24
25 125 evidence that the WGR rocks have been subducted into the mantle. The eclogite-facies
26
27 126 mineral assemblages have been pervasively overprinted by amphibolite and granulite-
28
29 127 facies parageneses associated with exhumation, decompression, partial melting and late
30
31 128 flattening and shearing (Wilks & Cuthbert, 1994; Labrousse *et al.* 2002; Hacker *et al.*
32
33 129 2010). However, the overprint was not total and fresh eclogite bodies are still frequent
34
35 130 across the WGR.

36
37
38
39 131 An exceptional effort in multi-method chronology during the past decades has
40
41 132 constrained the age of (U)HP metamorphism to between 425 and 400 Ma, i.e. during the
42
43 133 Scandian Orogeny (Hacker *et al.* 2010, and references therein). During this time, the
44
45 134 hyper-extended Baltic margin was buried beneath the Laurentian continental lithosphere
46
47 135 at rates of *c.* 5 mm yr⁻¹ (Cutts & Smit, 2018), ultimately reaching depths of 100 km or
48
49 136 more (Hacker *et al.* 2010 and references therein). The (U)HP stage was followed by
50
51
52 137 amphibolite-facies overprinting between 400-385 Ma (Terry *et al.* 2000; Kylander-Clark
53
54
55
56
57
58
59
60

138 *et al.* 2008; Krogh *et al.* 2011) and cooling below 400°C by *c.* 375 Ma (Hacker & Gans,
139 2005; Root *et al.* 2005; Walsh *et al.* 2013).

140 The WGR basement is bounded by the major Caledonide thrust complexes of the Middle
141 and Upper Allochthons. The Middle Allochthon comprises discrete lithotectonic units
142 that vary along the orogen. In southern Norway it is dominated by Proterozoic crystalline
143 complexes with metasediments, e.g. the Jotun Nappe Complex, Lindås and Jaeren
144 Nappes. In central and northern Sweden and northern Norway Caledonian high-grade
145 rocks, e.g., migmatite, granulite, metasediment, augen gneiss, amphibolite and eclogite
146 of the Seve and Kalak Nappe Complexes dominate (see e.g. Gee *et al.* 2013 and
147 references therein). The Middle Allochthon is interpreted to represent the distal
148 continental margin of Baltica and may include micro-continental fragments (Cuthbert *et*
149 *al.* 1983; Emmett, 1996; Andersen *et al.* 1991; Gee *et al.* 2010, 2013). The Upper
150 Allochthon contains a diverse assemblage of ophiolite and arc rocks that originated
151 outboard of Baltica within the Iapetus Ocean between 490-440 Ma (Stephens & Gee,
152 1985, 1989; Stephens, 1988).

153 Both allochthons underwent reworking and final emplacement onto the Baltican
154 continental margin during the Scandian collision. In addition, however, they show
155 evidence of earlier tectonometamorphic episodes. In the large Seve Nappe Complex in
156 Sweden, as well as in small slivers of allochthonous rocks in southwesternmost Norway,
157 this is indicated by (U)HP metamorphism at *c.* 460 – 445 Ma, which has been attributed
158 to a pre-Scandian arc-continent collision (e.g. Brueckner *et al.* 2004; Brueckner & Van
159 Roermund, 2004, 2007; Smit *et al.* 2010; 2011; Majka *et al.* 2012, 2014; Root & Corfu,
160 2012; Grimmer *et al.* 2015; Klonowska *et al.* 2016, 2017; Fassmer *et al.* 2017). Yet older,

1
2
3 161 c. 500-485 Ma, (U)HP metamorphic rocks are also recognized in the Seve Nappe
4
5 162 Complex of northern Sweden (Mørk *et al.* 1988, Root & Corfu, 2012, Barnes *et al.*
6
7 163 2019).

8
9
10 164 In the foreland regions of southern Norway, and central and northern Sweden an
11
12 165 additional nappe complex, the Lower Allochthon, underlies the Middle Allochthon and
13
14 166 comprises thrust repetitions of basement and sedimentary cover derived from the
15
16
17 167 Fennoscandian shield (hereafter termed the Baltican basement). These rocks record the
18
19 168 long-lived thrusting of the allochthons onto the Baltic margin during the Scandian.

20
21 169 Outcropping within the high-grade sections of the Baltican basement in the WGR are
22
23 170 belts (inliers) of more diverse lithological assemblages including psammitic and pelitic
24
25 171 metasediments, anorthosites and distinctive megacrystic augen gneisses. Such
26
27 172 assemblages may represent basement-cover repetitions derived from the Baltica slab (i.e.
28
29 173 Lower Allochthon), although they commonly also exhibit lithological similarities with
30
31 174 the Middle Allochthon in the main allochthon exposures (Krill, 1980; Robinson, 1995;
32
33 175 Robinson *et al.* 2014).

34
35
36
37 176 These inliers of the allochthons are conventionally regarded as being above the main
38
39 177 mass of orthogneisses in the tectonostratigraphy and down-folded into these (Krill, 1985;
40
41 178 Tucker *et al.* 2004; Robinson & Hollocher, 2008). The complete sequence is (from base
42
43 179 to top above the Baltican basement) the Risberget nappe (augen orthogneisses,
44
45 180 anorthosites, metagabbros); Sætra Nappe (quartzite with deformed dykes of
46
47 181 metadolerite); Blåhø Nappe (high grade metapelite, calc-silicate, marble, amphibolite and
48
49 182 mafic granulite); Støren Nappe (ophiolitic and arc rocks of greenschist to low
50
51 183 amphibolite facies). The last of these is part of the Upper Allochthon, while the others are
52
53
54
55
56
57
58
59
60

1
2
3
4
5
6
7
8
9
10
11
12
13
14
15
16
17
18
19
20
21
22
23
24
25
26
27
28
29
30
31
32
33
34
35
36
37
38
39
40
41
42
43
44
45
46
47
48
49
50
51
52
53
54
55
56
57
58
59
60

184 correlated with the Middle Allochthon. The Blåhø Nappe is correlated with the high-
185 grade Middle Seve Nappe in the main allochthon outcrop in central and northern Sweden.
186 Their structural evolution has been established in the north-eastern WGR in the
187 Trollheimen-Trondheim district (Robinson *et al.* 2014), where tectonostratigraphic units
188 of the Middle Allochthon were thrust over the Baltican basement, then this combined
189 sequence was folded to form a basement cored nappe that was translated eastwards
190 towards the foreland along the late, out-of-sequence, Storli Thrust. The nappe core
191 contains eclogite dated at 425 ± 10 Ma (Beckman *et al.* 2013), but the lower basement
192 unit below the thrust is devoid of eclogite. The same sequence can be traced to
193 Moldefjord and the southern part of the Nordøyane, far to the west (Fig. 1; see also
194 Robinson, 1985). A similar structural evolution was demonstrated by Young (2018) in
195 the central WGR, where allochthonous rocks ('mixed rocks') were tectonically
196 imbricated and infolded following emplacement onto the Baltica basement along major
197 foreland-vergent shear zones.

198 The allochthons have also been mapped out eastwards into the main allochthon outcrop
199 in the frontal zone in central Sweden (e.g. Gee *et al.* 2010). Here, the Middle Allochthon
200 is more continuously exposed, is several km thick and bounded by major thrusts. In the
201 WGR, however, these nappes are either extremely attenuated to a few meters in thickness
202 or excised entirely (Robinson, 1995). In the Trondheim area and southwestwards to
203 Moldefjord the upper boundary of the Middle Allochthon against the Upper Allochthon is
204 a major west-vergent, late orogenic ductile detachment fault, the Agdenes Detachment
205 (Robinson *et al.* 2014).

206

207 **2a. Nordøyane ultra-high pressure domain**

208 The sample investigated here comes from the island of Fjørtoft (Fig. 1b) in the
 209 Nordøyane archipelago, immediately west of Moldefjord, which lies within the
 210 northernmost UHP domain of the WGR (Root *et al.* 2005). The Middle Allochthon
 211 sequence established in the Trollheimen-Moldefjord area has been mapped across the
 212 Nordøyane by Terry & Robinson (2003, 2004). The lithology of interest is a pelitic
 213 garnet-kyanite gneiss in an assemblage also including biotite-garnet migmatite, calc-
 214 silicate, marble and eclogite, all correlated with the Blåhø Nappe. The structural and
 215 fabric evolution in the Nordøyane provides key constraints in the interpretation of the
 216 zircon dating set out in the following sections.

217 There are two major structural domains in Nordøyane (Terry & Robinson, 2013, 2014)
 218 separated by a major late-orogenic, steep sinistral discontinuity, the Åkre-Midøy shear
 219 zone. To its south the structural evolution resembles the situation in Trollheimen and
 220 Moldefjord. The northern structural domain has been brought in against the southern
 221 domain from the NE by motion along the Åkre-Midøy shear zone (Terry & Robinson,
 222 2003, 2004). Evidence for UHP metamorphism is found in the Baltican basement, the
 223 allochthons and in mantle-derived ultramafic massifs (Dobrzhinetskaya *et al.* 1995; Terry
 224 *et al.* 2000; Carswell *et al.* 2006; Vrijmoed *et al.* 2006; Spengler *et al.* 2009; Butler *et al.*
 225 2013). The Middle Allochthon is only represented by the Blåhø Nappe, which has been
 226 folded into the core of a large recumbent, isoclinal synform with dioritic to granitoid
 227 gneisses of the Baltican basement on either limb (Terry & Robinson, 2004). The contact
 228 is coincident with an eclogite- (or high-P granulite-) facies shear zone that extends
 229 through Blåhø and a few hundred meters into the adjacent basement, and in which

1
2
3 230 mylonite lineations and rotated porphyroclasts show top-SE shear sense when the folds
4
5 231 are restored to pre-folding geometry (Terry *et al.* 2000a; Terry & Robinson, 2004). These
6
7 232 fabrics are associated with transformation of two metagabbro lenses to eclogite (Mørk,
8
9 233 1985; Terry & Robinson, 2004) dated at 410 ± 2 Ma (Krogh *et al.* 2011; see also Mørk &
10
11 234 Mearns, 1986). Terry *et al.* (2000a) and Terry & Robinson (2004) proposed that this
12
13 235 shear zone emplaced the UHP Blåhø Nappe over Baltican basement that had only
14
15 236 experienced HP eclogite conditions, but Carswell *et al.* (2006) showed that nearby
16
17 237 eclogites in the Baltican basement equilibrated under UHP conditions, in which case the
18
19 238 shear zone operated during exhumation and the metamorphic assemblages are retrograde.
20
21 239 It remains possible, however, that all the UHP eclogites are part of the sheared basement
22
23 240 pediment attached to the underside Blåhø Nappe and a cryptic HP basement unit lies at a
24
25 241 deeper structural level.
26
27 242 Lenses of garnet peridotite and pyroxenite derived from subcontinental mantle decorate
28
29 243 the basement-cover contact and are scattered through the Baltica basement in a zone a
30
31 244 few hundred meters below it, confirming the existence of a fundamentally important
32
33 245 tectonic contact here. Late fabrics defined by UHP mineral assemblages in these garnet
34
35 246 pyroxenites at Bardane, Fjortoft and Flemsøy give $P \approx 6$ GPa at sub-geotherm
36
37 247 temperatures for cratonic mantle (e.g. Vrijmoed, van Roermund & Davies, 2006;
38
39 248 Scambelluri, van Roermund & Pettke, 2010). A mineral isochron age of 429 ± 3.1 Ma for
40
41 249 this mineral assemblage was interpreted to represent an early stage in the subduction of
42
43 250 the outermost Baltica continental margin (Spengler *et al.* 2009).
44
45 251 Two kyanite eclogites from the Blåhø Nappe very close to its lower boundary record P-T
46
47 252 conditions overlapping the diamond stability field (Terry *et al.* 2000) and one of these
48
49
50
51
52
53
54
55
56
57
58
59
60

253 gives a Lu-Hf mineral age of 404.9 ± 7.9 Ma (Cutts & Smit, 2018). A distinctive feature
 254 of the Blåhø in the Nordøyane and Moldefjord area is that eclogites and other mafic rocks
 255 are a common part of the rock assemblage, while these are less common in the main
 256 outcrop of the equivalent Seve Nappe in Sweden. An eclogite from the island of Gossa,
 257 adjacent to Fjørtoft, gives a Scandian Sm-Nd mineral isochron age of 413.9 ± 3.7 Ma
 258 (Kylander-Clarke, 2009). Another two from the mainland along strike from Nordøyane
 259 have given Scandian ages for (U)HP metamorphism (418 ± 27 Ma, Tverfjell north of
 260 Molde; Griffin & Brueckner, 1985 and 415.2 ± 0.6 Ma, Averøya, near Kristiansund;
 261 Krogh *et al.* 2011).
 262 The age of UHP metamorphism in the Baltican basement in the northern domain is
 263 constrained by a U-Pb zircon date of 405 ± 1 Ma from an eclogite at Midsund, Otrøy
 264 (Krogh *et al.* 2011) although, puzzlingly, Kylander-Clark *et al.* (2007) derived Lu-Hf
 265 garnet and Sm-Nd garnet – whole-rock ages for this eclogite of 380 ± 14 Ma and 388
 266 ± 10 Ma, respectively, which are significantly younger than any other UHP eclogite ages
 267 in the WGR; they are, however, Scandian. Zircons from the Svartberget microdiamond-
 268 bearing metasomatic veins in garnet websterite within Baltican basement orthogneiss
 269 give a robust U-Pb (LA-ICP-MS) age for a cluster of concordant points of 410.6 ± 2.6
 270 Ma (Quas-Cohen, 2013) which is taken to date metasomatism and microdiamond
 271 formation. Samples from the same body also yielded significantly younger and perhaps
 272 less robust dates by U-Pb on zircon using ID-TIMS, which gave a discordia intercept of
 273 397.2 ± 1.2 Ma (Vrijmoed *et al.* 2013) and Sm-Nd mineral isochrons yielded dates of 393
 274 ± 3 Ma to 381 ± 6 Ma (Vrijmoed *et al.* 2008) interpreted to be cooling ages.

1
2
3
4
5
6
7
8
9
10
11
12
13
14
15
16
17
18
19
20
21
22
23
24
25
26
27
28
29
30
31
32
33
34
35
36
37
38
39
40
41
42
43
44
45
46
47
48
49
50
51
52
53
54
55
56
57
58
59
60

Overall, it is possible to reconstruct an evolution for this northern, UHP domain, based on the tectonic model of Terry & Robinson (2004) in Nordøyane and adjacent areas:

- 1) The Blåhø Nappe is emplaced on to the Baltica basement (time uncertain but before 430 Ma).
- 2) Baltica basement and Blåhø Nappe are subducted deep enough to capture mantle ultramafic rocks (at least 200 km) at ~430 Ma during the early stages of the Scandian continent-continent collision.
- 3) UHP eclogites form, or continue to equilibrate, in both units until ~410 Ma.
- 4) The Blåhø Nappe and a detached pediment of Baltica Basement rise as a nappe over the (still descending?) deeper basement, generating the top-southeast HP eclogite or HP granulite shear fabrics (≤ 410 Ma).

The available evidence favours a common, roughly synchronous, Scandian diamond-eclogite facies metamorphism for both the Blåhø Nappe and the Baltica basement in the northern domain of Nordøyane, with a basement-cover nappe similar in geometry to the Trollheimen-Moldefjord region but operating at much deeper levels. The whole basement-cover package in both northern and southern structural domains has then been refolded about upright, folds associated with a pervasive, sinistral or top-west amphibolite-facies fabric with horizontal lineations and fold axes (Terry & Robinson, 2003) dated at 396 Ma from boudin-neck pegmatites (Krogh *et al.* 2011). (U)HP lithologies and fabrics are preserved only as rare relics where they have survived overprinting by the late-orogenic deformation. Any signature of pre-Scandian metamorphism must have survived both this and the Scandian UHP tectono-metamorphism.

298

299 **3. Sample Description**

300 The sample investigated here was collected from an old quarry at Vågholmane, just north
301 of the ferry terminal. It is the residue of the same sample (ID: Fj-19; Fig. 2) from which
302 Dobrzhinetskaya *et al.* (1995) extracted metamorphic diamond by a chemical dissolution
303 process performed on a crushed block. The lithology has been described previously by
304 Dobrzhinetskaya *et al.* (1995), Holder *et al.* (2015), Liu & Massonne (2019) and Terry *et al.*
305 (2000b); the latter's sample (recoded by them as UHP1) was a thin section cut from
306 the microdiamond-bearing sample, so is the same sample block from which our zircons
307 were sourced. It is composed of garnet, kyanite, phlogopite, K-feldspar, plagioclase,
308 quartz, graphite and additionally rutile, sulphides, monazite and zircon. Garnet is
309 abundant, pale mauve-coloured, typically 0.5-1.0 cm in size, and locally occurs as
310 globular megacrysts of 3-5 cm surrounded by conspicuous coronas of felsic minerals. It
311 shows distinctive zoning with low Ca garnet cores (Terry *et al.* 2000b; Holder *et al.*
312 2015; Liu & Massone, 2019; authors' unpublished data) enclosing abundant, small
313 needles of kyanite. High Ca rims contain larger inclusions of kyanite, quartz, rutile,
314 graphite, perthitic feldspar and sulphides, along with rationally orientated needles of
315 rutile. It has not often been recognised that the rock is a blastomylonite with streaky
316 appearance suggesting pre-tectonic migmatization. Relics of granitic (partial) melt are
317 preserved as embayments and inclusions in the garnet rims and are composed of perthite,
318 quartz and phlogopite. Monazite and zircon are found in both cores and rims of garnet.
319 The rock matrix is generally composed of fine-grained plagioclase and K-feldspar (from
320 the breakdown of coarse perthite and garnet), quartz and large flakes of phlogopite and

1
2
3
4
5
6
7
8
9
10
11
12
13
14
15
16
17
18
19
20
21
22
23
24
25
26
27
28
29
30
31
32
33
34
35
36
37
38
39
40
41
42
43
44
45
46
47
48
49
50
51
52
53
54
55
56
57
58
59
60

graphite. No microdiamond has yet been found in-situ, nor any other (U)HP phases, although muscovite inclusions in garnet associated with phlogopite may be relics after phengite. Larsen *et al.* (1998), who described the rock as a ‘felsic granulite’, estimated $P = 16\text{--}23$ kbar at $600\text{--}800$ °C for the matrix assemblage assuming equilibrium with garnet rims. However, the recent detailed study by Liu & Massonne (2019) suggests that this rock underwent most probably a prolonged anticlockwise P-T path, with peak conditions around 1.35-1.45 GPa and 770-820 °C and an earlier equilibration event at *c.* 1.35-1.45 GPa and 770-820 °C.

In the field, two linear fabrics can be recognised in the Blåhø Nappe felsic gneisses (Terry *et al.* 2000; Terry & Robinson, 2004). The earlier fabric is represented by the sample UHP1 described above, and is defined by mineral-aggregate rods and common orientation of kyanite. Kinematic indicators on steep foliation surfaces including rotated kyanite and garnet porphyroclasts indicating north-side-up shear that translates to top-southeast shear when the effects of later folding are removed, as found in the eclogite-facies shear zones described above. Terry & Robinson (2004) attributed the tectonite fabrics of the basement metagabbros and dioritic orthogneisses to the same kinematic system as this early fabric in the Blåhø Nappe gneiss, suggesting that it operated at about 410 Ma, postdating an episode of partial melting, and was related to foreland directed transport of a (U)HP basement with associated Seve-Blåhø allochthon.

The later fabric is a mineral-aggregate rodding lineation defined by sillimanite replacing deformed, fish-shaped kyanite porphyroclasts or disseminated in the matrix, which displays extreme grain-size reduction. Garnet porphyroclasts are dismembered and strung out in the lineation (Terry *et al.* 2000b). Mica- and sillimanite-rich elements of the matrix

display S-C fabrics. The lineations and associated fold axes are roughly horizontal and the kinematic indicators show consistent top-west or sinistral shear. This fabric overprints and re-orientates the steeper kyanite lineation. This late top-west shear fabric also dominates large parts of the allochthons and some of the adjacent basement gneisses in the westernmost WGR, indicating a top-to-the-west transport. This was related to reversal of motion on the major thrust surfaces, the development of Agdenes Detachment and Nordfjord-Sogn Detachment Zone and the late-orogenic Old Red Sandstone basins (Norton, 1987; Wilks & Cuthbert, 1994; Brueckner & Cuthbert, 2013; Robinson *et al.* 2014; Young, 2018).

Zircons in the mineral separate that we obtained from sample Fj-19 contains micro-inclusions of quartz, feldspar, mica, apatite, graphite and rutile (H.-J. Massonne, pers. comm. 2005). No HP or UHP indicator micro-inclusions such as diamond, coesite, phengitic mica or jadeitic clinopyroxene have been found. Monazite from the microdiamond-yielding sample has been analysed by electron microprobe (Th-U-total Pb) and secondary ionization mass spectrometry (U-Th-Pb), along with a sample of porphyroclastic mylonite with the younger lineation from 1km west of Vågholmane (Terry *et al.* 2000; their samples UHP1 and 929, respectively). The analyses yield a cluster of dates between 1100 and 950 Ma, a few scattered dates between 900 Ma and 500 Ma, and other clusters at *c.* 415, 408, 395 Ma and *c.* 375 Ma. The older dates of 415.0 ± 6.8 Ma (SIMS) and 408.0 ± 5.6 Ma (EPMA) were obtained from the same monazite inclusions in garnet and have been interpreted as indicating the maximum age of garnet growth. The two youngest dates were interpreted to represent different phases of exhumation from deep subduction conditions. Recently, Holder *et al.* (2015) have also

1
2
3 367 performed *in-situ* monazite U-Th-Pb dating using laser ablation split stream inductively
4
5 368 coupled plasma mass spectrometry. These authors dated two samples of the same rock
6
7 369 and obtained the following results: a cluster of ages between 1200 and 900 Ma,
8
9
10 370 Caledonian concordia ages peaking at 431.1 ± 1.7 Ma, 426.8 ± 1.7 Ma, 425.5 ± 3.0 , 393
11
12 371 ± 3.0 Ma and 391.3 ± 2.7 Ma. Contrasting REE patterns for inclusions and matrix grains
13
14 372 dated at *c.* 425 Ma suggest that garnet growth took place at this time, but other inclusions
15
16 373 as young as *c.* 390 Ma may indicate either continued growth to this time or re-setting. A
17
18 374 continued growth of monazite is also suggested by Liu & Massonne (2019), who reported
19
20 375 Th-U-total Pb monazite dates spanning from 460 to 380 Ma and interpreted them to
21
22 376 reflect a prolonged residence time under relatively high temperatures due to two burial
23
24 377 events that have never reached UHP conditions. We differ by not ruling out diamond-
25
26 378 stable P-T conditions at some time during its history, as some stages of the rock history
27
28 379 may have been destroyed during overprinting, for example during partial melting.
29
30
31 380 To our knowledge, no zircon dates have so far been documented in the literature for this
32
33 381 unusual and widely studied rock.
34
35
36
37
38
39

40 383 **4. Methods**

41
42 384 Uranium-lead dating was performed on zircon grains initially separated by D. A.
43
44 385 Carswell and H.-J. Massonne for studies of inclusions; the separate was kindly provided
45
46 386 by H.-J. Massonne, who mounted and polished the grains in an epoxy mount. The zircon
47
48 387 grains are from the same rock volume from which micro-diamond was isolated
49
50 388 (Dobrzhinetskaya *et al.* 1995). The grains are 100-250 μm in length and were polished to
51
52 389 their geometric core. U-Pb dating of zircon was performed at the Swedish Museum of
53
54
55
56
57
58
59
60

Natural History, Stockholm, using a Nu Instruments Plasma II multi-collector inductively coupled plasma mass spectrometry (MC-ICPMS) instrument coupled to an ESI NWR193UC excimer laser ablation system. The m/z (mass-to-charge ratio) corresponding to masses 202, 204, 206, 207 and 208 were measured on ion counters, and those corresponding to 232, 235, and 238 were measured on Faraday collectors. The laser was fired for 35 s with a fluence of 3.5 J/cm², a pulse rate of 8 Hz and a spots size of 15 μ m. Helium was used as a sample carrier gas (0.3 l/min) to flush the laser cell and was mixed with argon sample gas (0.9 l/min) before entering the ICP-MS. Analyses were corrected for mass bias and elemental fractionation using the protocols of Kooijman *et al.* (2012). The 91500 zircon reference material (1065 Ma; Wiedenbeck *et al.* 1995) was used for normalization and repeated analyses indicated external reproducibility of 1.0% 2RSD for the ²⁰⁷Pb-²⁰⁶Pb age and 1.2% 2RSD for the ²⁰⁶Pb-²³⁸U age (n = 58). Accuracy was assessed by analysing the secondary reference zircons Plešovice (337 Ma; Sláma *et al.* 2008), GJ-1 (609 Ma; Jackson *et al.* 2004) and Temora 2 (417 Ma; Black *et al.* 2004). We obtained 336 ± 11 Ma (Plešovice; n = 8), 606 ± 3 Ma (GJ-1; n = 8), and 416 ± 9 Ma (Temora 2; n = 5), all of which agree within 1% of published age estimates for these materials. Data reduction employed in-house Excel macros. Age calculations and construction of concordia diagrams were prepared using the Excel extension Isoplot 3.75 (Ludwig, 2012). All uncertainties are reported at the 2 σ level. Age data are illustrated in Figure 4 and presented in Table 1.

5. Results

1
2
3
4
5
6
7
8
9
10
11
12
13
14
15
16
17
18
19
20
21
22
23
24
25
26
27
28
29
30
31
32
33
34
35
36
37
38
39
40
41
42
43
44
45
46
47
48
49
50
51
52
53
54
55
56
57
58
59
60

Separated zircon grains are spherical or slightly elongated in shape, with rounded edges. Cathodoluminescence (CL) images reveal complex internal structure and most zircons display obvious multi-stage growth features (Fig. 3). Most commonly, zircon grains display cores with well-defined concentric oscillatory zoning, typical of magmatic zircon, which is overgrown by a bright-CL rims. Such rims show no visible zoning and are likely of metamorphic origin. U-Pb isotope data obtained from the dated grains are presented in Table 1 and reveal a complex multi-component age signature. The majority of dates older than 700 Ma were obtained from zircon cores and display significant degrees of discordance (Figs. 4a, d, f). Several ^{207}Pb - ^{206}Pb date clusters can be distinguished among the obtained results: (1) a Neoarchean cluster between 2.8-2.5 Ga ($n = 6$); (2) a small cluster in the Mesoproterozoic (1.5-1.3 Ga; $n = 3$); (3) late Mesoproterozoic to early Neoproterozoic dates between 1.1-0.9 Ga ($n = 6$); and (4) a group of Neoproterozoic dates between 0.9-0.7 Ga ($n = 7$). A small group of three concordant dates between 540-520 Ma (Table 1) was also obtained, one of which is from a core domain, whereas the other two were obtained from rims. A notable number of Caledonian spot dates range from 450 to 400 Ma (Fig. 4b). Two subgroups of dates can be distinguished among the concordant results (Fig. 4e). Five of the oldest Caledonian dates cluster between 450-440 Ma and give a concordia age of 446.6 ± 2.1 Ma (Fig. 4c). Another cluster of concordant dates is observed between 437-423 Ma, and yield a weighted average ^{206}Pb - ^{238}U date of 428.3 ± 1.7 Ma. The three youngest dates are *c.* 415 Ma and younger.

6. Discussion

6.a. Provenance and exotic nature of the Fjortoft diamondiferous gneiss

1
2
3 435 The oldest detrital ages (2.8-2.5 Ga) are not known from the Baltica basement rocks of
4
5 436 the WGR. Such detrital ages are, however, observed in the Lower and Middle
6
7 437 Allochthons in Sweden (e.g. Gee *et al.* 2014, 2015; Ladenberger *et al.* 2014), as well as
8
9 438 in southwesternmost Norway (Smit *et al.* 2011). Two younger groups, 1.5-1.3 Ga and
10
11 439 1.1-0.9 Ga, correspond to the Gothian and Sveconorwegian orogenies, respectively. The
12
13 440 older group is widespread in the WGR and marks a major episode of magmatism within
14
15 441 the Fennoscandian basement (e.g. Corfu & Andersen, 2002; Tucker *et al.* 2004; Krogh *et*
16
17 442 *al.* 2011). The younger group is also common across the WGR, both in the allochthons
18
19 443 and in the basement; it derives from magmatism and metamorphism during the
20
21 444 Sveconorwegian Orogeny (e.g. Tucker *et al.* 1990; Bingen & van Breemmen, 1998;
22
23 445 Bingen *et al.* 2001; Røhr *et al.* 2004; Walsh *et al.* 2007; Des Ormeau *et al.* 2015; Corfu &
24
25 446 Andersen, 2002). Terry *et al.* (2000) recognised a similar group of ages among monazite
26
27 447 cores from the diamond-bearing gneiss on Fjortoft. These age components clearly
28
29 448 establish the Baltic provenance of this rock, indicating that its sedimentary protolith was
30
31 449 deposited within the Baltic continental realm or its Iapetus Ocean margin.
32
33 450 Neoproterozoic ages between 0.9 and 0.7 Ga are less common within the Baltic basement
34
35 451 (Bingen & Solli, 2009). They are, however, reported from detrital zircons in the Seve
36
37 452 Nappe Complex in Sweden (Gee *et al.* 2014) and igneous bodies of similar age are also
38
39 453 known from other parts of the Middle Allochthon. Paulsson & Andréasson (2002)
40
41 454 reported *c.* 845 Ma U–Pb age of the Vistas granite in the Seve Nappe Complex in
42
43 455 northern Sweden, while *c.* 840 and 710 Ma ages are typical of granitic magmatism in the
44
45 456 Sørøy-Seiland and Havvatnet nappes of the Kalak Nappe Complex in northernmost
46
47 457 Norway (Kirkland *et al.* 2006). Walker *et al.* (2016) have also reported a *c.* 725-700 Ma
48
49
50
51
52
53
54
55
56
57
58
59
60

1
2
3
4
5
6
7
8
9
10
11
12
13
14
15
16
17
18
19
20
21
22
23
24
25
26
27
28
29
30
31
32
33
34
35
36
37
38
39
40
41
42
43
44
45
46
47
48
49
50
51
52
53
54
55
56
57
58
59
60

tectonothermal event recorded in the Caledonides of Shetland. Several of these possible sources derive from Neoproterozoic magmatism and tectonism (Renlandian and Knoydartian) whose products subsequently involved in the northern Iapetus-Caledonide cycle (Cawood *et al.* 2010). The exact source of zircons with 0.9-0.7 Ga ages in the Fjørtoft sample remains unresolved, but it is clear that these data represent an exotic component acquired when the sedimentary protolith was located in a palaeogeographic location distal to the Baltic craton.

A similar explanation may be proposed for the small group of 540 to 520 Ma ages, which were also obtained by Terry *et al.* (2000), but left them uninterpreted. The dates are concordant and form a distinct cluster, indicating that they have geological meaning. Components of similar age are extremely rare in the present-day Scandinavian Caledonides, and are mainly restricted to the Kalak Nappe Complex (e.g. Roberts *et al.* 2010). Interestingly, dates in the range 650-500 Ma are rare but persistently found in the mantle-derived ultramafic rocks and enclosed eclogite in Nordøyane (Jamtveit *et al.* 1991; Spengler *et al.* 2009) and in the central WGR (Medaris *et al.* 2018), suggesting magmatism or tectonism in the Iapetus realm during this interval that may have also had a crustal expression.

The spectrum of different age populations further distinguishes the Fjørtoft gneiss from the adjacent basement orthogneisses and confirms its profoundly allochthonous nature and reinforces its correlation with the Seve-Blåhø Nappe. Moreover, it suggests a previously unrecognised link between this lithotectonic unit and the terranes of the north-Norwegian and Swedish Caledonides.

480

6.b. Caledonian ages and evidence for double-dunking

U-Pb zircon dates from the Fjærtøft gneiss corresponding to the span of the Caledonian orogenic cycle cluster around *c.* 447 Ma and *c.* 437-423 Ma with three younger dates $\leq c.$ 415 Ma. The oldest age of these mentioned above was not identified in published monazite age studies by Terry *et al.* (2000b) or Holder *et al.* (2015). This age is significantly earlier than almost all previous higher-precision ages for (U)HP-HT metamorphism in the WGR.

This Ordovician age peak may be compared with dates in other outcrops of the allochthons in the WGR. Zircon U-Pb dates of 470-430 Ma were reported for eclogites in allochthonous units (Blåhø Nappe?) in the western and eastern-central parts of the WGR but were attributed to protolith ages (Walsh *et al.* 2007 - discordant dates; DesOrmeau *et al.* 2015). We speculate that these are lower Palaeozoic metavolcanics similar to the layered eclogites described in the Blåhø Nappe on Fjærtøft by Terry & Robinson (2004) and on the mainland north of Molde by Carswell & Harvey (1985). Walsh *et al.* (2007) also reported a protolith (detrital?) zircon age of 480 ± 12 Ma from a pelite in the Blåhø Nappe. However, our zircon ages are clearly metamorphic and do not represent growth in magmatic protoliths. In contrast, Gordon *et al.* (2016) presented U-Pb zircon age populations of *c.* 467 and *c.* 439 Ma obtained from leucosomes in metapelites of the Seve-Blåhø Nappe north of Trondheim, which they interpreted to represent (U)HP zircon growth and subsequent migmatization.

The younger of our two larger Caledonian U-Pb zircon age-peaks matches well with the timing of Ca-rich garnet rims as indicated by *in-situ* monazite ages of *c.* 425 Ma and perhaps as old as 430 Ma, (Holder *et al.* 2015) corresponding to an episode of

1
2
3
4
5
6
7
8
9
10
11
12
13
14
15
16
17
18
19
20
21
22
23
24
25
26
27
28
29
30
31
32
33
34
35
36
37
38
39
40
41
42
43
44
45
46
47
48
49
50
51
52
53
54
55
56
57
58
59
60

migmatismation evidenced by granitic melt **inclusions** enclosed in Ca-rich garnet rims. It is also not much younger than the earliest ages attributed to Scandian subduction of the Baltica margin around **430 Ma** as indicated by garnet pyroxenites in mantle-derived ultramafites in Nordøyane (Jamtveit *et al.* 1991; Spengler *et al.* 2009) and elsewhere (Medaris *et al.* 2018). These ages are all significantly older than the timing of HP-eclogite facies SE-vergent shearing involving the metagabbros in Nordøyane (Terry *et al.* 2000a; Terry & Robinson, 2004) at $410 \pm 2\text{Ma}$ (Krogh *et al.* 2011) which has been correlated with the SE-vergent shear overprinting the migmatite fabric in the Fjortoft gneiss. This puts a younger age bracket on the duration of migmatismation. Also, ages around 410 Ma are relatively scarce in our dataset, suggesting that during this foreland-directed shearing little new zircon was generated, and/or there was little resetting of the zircon U-Pb isotopic system.

The late Ordovician age components in our dataset (**c. 447 Ma**) are uncommon or absent in the WGR, but widely recognised within the Seve Nappe Complex of Jämtland in Sweden and in tectonic slivers of probable Middle Allochthon rocks in southwesternmost Norway (e.g. Brueckner *et al.* 2004; Brueckner & van Roermund, 2007; Smit *et al.* 2011; Majka *et al.* 2012; Root & Corfu, 2012; Ladenberger *et al.* 2014; Grimmer *et al.* 2015; Klonowska *et al.* 2017; Fassmer *et al.* 2017). These terranes record a mid- to late Ordovician episode of (U)HP metamorphism. The lithologies in the Åreskutan Nappe, Middle Seve Nappe in Jamtland, central Sweden are similar to the Fjortoft gneiss in that they are metapelitic sillimanite or kyanite-bearing migmatites that record a pre-migmatite, diamond-stable UHP metamorphism. Granulite-facies metamorphism and migmatismation has been dated at c. 439 Ma during decompression and partial melting,

following UHP metamorphism at *c.* 455 Ma (Majka *et al.* 2012). Emplacement of these rocks as a hot nappe above the Lower Seve Nappe Complex was dated from monazite in basal mylonites at 424 ± 6 Ma (Majka *et al.* 2012) which was within error of the age for crystallisation of post-migmatite, pre-mylonite pegmatites during nappe emplacement at *c.* 430-428 Ma (Ladenberger *et al.* 2014). The close correspondence of the age for this migmatisation with the earliest Caledonian ages from the Fjortoft gneiss encourages the tentative proposal that migmatisation took place there, too, at that time. While this may be true, the *c.* 430-428 Ma age for pegmatite intrusion at Åreskutan during Scandian nappe emplacement corresponds closely to the evidence for growth of high-Ca garnet rims in the Fjortoft gneiss around 430-425 Ma (Holder *et al.* 2015), which we attribute to partial melting. This suggests that partial melting of the Fjortoft gneiss took place during the earliest phase of exhumation of the far-western, Blåhø segment of the Seve Nappe Complex. If two episodes of partial melting took place in these rocks (late Ordovician and mid-Silurian), evidence must have been obscured by the subsequent intense ductile shearing. If the Blåhø Nappe in western Norway can be directly correlated with the Seve Nappe Complex in central Sweden, the evidence that the Blåhø Nappe, and possibly a sheared pediment of Baltica basement orthogneisses, was still moving forelandwards around 410 Ma suggest deformation at the base of the Åreskutan Nappe transferred to a deeper structural level soon after *c.* 425 Ma.

The interpretations above, based on geological evidence and previous geochronological studies, suggests that partial melting may have been significant in generating the zircon U-Pb age pattern. If representative of the rock, the 447 Ma and 437-423 Ma zircon age clusters probably represent discrete stages in which new zircon formed. This may have

involved complete neocrystallization and/or re-crystallisation of pre-existing zircon. The latter is common in (U)HP granulites in other collisional orogens (e.g., Bröcker *et al.* 2010), as well as in ultra-high temperature (UHT-HT) rocks (e.g., Mezger & Krogstad, 1997; Kooijman *et al.* 2010), where partial melting was an important process. In the Fjortoft rocks there was an apparent cessation in zircon crystallisation (or neocrystallisation) during a period of *c.* 15 Ma, which also requires explanation.

Zircon crystallisation in felsic rocks can take place following an excursion beyond the solidus (Yakymchuk & Brown, 2014), either by transient decompression or heating or both. The following two options are hence proposed for the interpretation of the 447 and 437-423 Ma age clusters: (1) they postdate two distinct cycles of high-grade, possibly kyanite-stable high temperature (HT) metamorphism - one before 447 Ma and the other before 423 Ma; (2) they bracket two thermal excursions beyond, and back to, the solidus during a single protracted stage of possibly kyanite-stable HT metamorphism. Regardless of which of the two options proves true or which of these may be associated with micro-diamond growth, the history and context of the rocks, as set out in the foregoing text, requires at least one pulse of pre-Scandian metamorphism.

Previously published ages derived from the (U)HP eclogites in the Nordøyane and adjacent region in the WGR, mainly in the range 415-400 Ma, are only represented in our dataset by one concordant date of *c.* 415 Ma and a slightly discordant, similar date (Fig. 4b). The presence of Scandian UHP eclogites in the basal parts of the Blåhø Nappe in Nordøyane (404.9 ± 7.9 Ma; Cutts & Smit, 2018) suggests that the Blåhø Nappe of Fjortoft underwent Scandian, perhaps diamond-stable, UHP metamorphism. This apparently resulted in very little new zircon growth or re-crystallisation in the sample

1
2
3 573 examined here. Scandian UHP eclogite formation in the allochthons and Baltica
4
5 574 basement evidently continued well after migmatisation of the Blåhø metapelitic gneisses
6
7
8 575 such as those at Fjortoft (there is evidence that gneisses in this area underwent partial
9
10 576 melting during UHP metamorphism; see e.g. Vrijmoed *et al.* 2013; Quas-Cohen, 2013).
11
12 577 The single concordant metamorphic zircon date at *c.* 396 Ma is identical within error with
13
14 578 a cluster of U-Th-Pb ages for matrix monazites in the Fjortoft gneiss (Terry *et al.* 2000b).
15
16
17 579 This also closely corresponds to a regionally-distributed suite of titanite U-Pb ages
18
19 580 (Tucker *et al.* 1991) interpreted to date a widespread cessation of Pb loss during
20
21 581 exhumation of the WGR from below the major extensional Agdenes Detachment (Tucker
22
23 582 *et al.* 2004). The late horizontal lineation and sinistral shear fabric in northern Fjortoft
24
25 583 may be attributed to this late-Scandian tectonism.
26
27
28 584 The zircon U-Pb dataset presented here demonstrates an early Caledonian, pre-Scandian
29
30 585 metamorphic event in the northwestern WGR that corresponds to a mid-Ordovician to
31
32 586 early Silurian subduction episode recorded in the main outcrop of the Seve Nappe. The
33
34 587 evidence for coeval Scandian UHP metamorphism of the Blåhø Nappe and in the Baltica
35
36 588 basement in Nordøyane (and probably more widely in the WGR) strongly suggests that
37
38 589 both underwent subduction in the late Silurian and early Devonian, and thus a ‘double-
39
40 590 dunk’ for the Blåhø-Seve Nappe of Fjortoft.
41
42
43
44 591 The ‘double-dunk’ hypothesis (Brueckner & Van Roermund, 2004; Brueckner, 2006)
45
46 592 predicts both subduction and eduction of a continental margin, so evidence is required for
47
48 593 an episode of exhumation of the subducted slab between any two ‘dunks’; if this is
49
50 594 lacking it is difficult to refute a single, prolonged subduction episode. In the WGR,
51
52 595 evidence for pre-Scandian tectonism and metamorphism has been effectively obliterated
53
54
55
56
57
58
59
60

1
2
3
4
5
6
7
8
9
10
11
12
13
14
15
16
17
18
19
20
21
22
23
24
25
26
27
28
29
30
31
32
33
34
35
36
37
38
39
40
41
42
43
44
45
46
47
48
49
50
51
52
53
54
55
56
57
58
59
60

by Scandian deformation and overprinting. All that can be deduced is that assembly of the Middle Allochthon nappe stack and its emplacement onto the Baltica basement was the earliest discernable event (e.g. Robinson *et al.* 2014). However, petrological evidence for migmatisation during decompression in the correlative Åreskutan Nappe in the foreland Seve Nappe Complex (Majka *et al.* 2012; Klonowska *et al.* 2014) shows that the Seve Nappe did, at least partially, exhume following the Ordovician subduction event, but before the Scandian subduction and climactic collision. The distribution of concordant ages in our U-Pb zircon dataset, while showing clear clustering at specific time intervals, does indicate some continuity of Caledonian zircon generation, which may be due to incomplete exhumation after the first dunk and stalling at fairly deep, hot crustal levels during the relatively brief interval before the Scandian dunk. Overall, the age pattern from our new geochronological evidence for the Middle Allochthon within the WGR is consistent with the predictions of the dunk tectonics model.

The sample from which our zircon set was separated has been iconic in UHP metamorphic studies since the discovery of microdiamonds within it by Dobrzhinetskaya *et al.* (1995), as this was the first metamorphic microdiamond find in the Caledonides and one of the first globally. Yet, this sample remains enigmatic because no microdiamond has yet been found *in-situ* within it. The demonstration of multiple metamorphic events in this rock, of which two are probably high- or ultrahigh- grade, begs the question of the genesis of the diamonds, although this is challenging because of their lack of petrographic context. The possible double-dunk scenario for the Fjortoft gneiss set out above permits that these rocks passed through diamond-stable physical conditions twice during the Caledonian cycle. Hence, a priority for future work is to find the

microdiamonds *in-situ*, although several workers have already made great efforts to do this. A possible barrier to success is the late structural-metamorphic overprint that this belt of Blåhø has suffered, so future efforts might be better focused on adjacent areas where this overprint is less complex and intense.

Finally, it is worth noting the comparison between the zircon dates presented above and previously published monazite dates (Terry *et al.* 2000b; Holder *et al.* 2015; Liu & Massonne, 2019), which reinforce the common observation that zircon and monazite age records are complementary and that both only rarely provide the same age results, and represent the same petrological process, in a single rock (Kooijman *et al.* 2017).

7. Conclusions

(1) The diamond-bearing gneiss from Fjørtoft in the Nordøyane UHP domain of the Western Gneiss Region contains detrital zircon cores that reveal Baltic provenance. This is consistent with previously proposed affinity of the studied gneiss to the Seve-Blåhø Nappe of the Middle Allochthon. A few Archean ages are, however, clearly exotic in respect to the local basement of the WGR directly underlying the studied gneiss. Thus, a more exotic source is required for these zircons both at Fjørtoft and in the other diamond-bearing gneisses of the Seve Nappe Complex.

(2) At least two distinct high-grade metamorphic events preceding the final stage of the Scandian collision are recorded by the diamond-bearing gneiss from Fjørtoft: (1) at 446.6 ± 2.1 Ma; and (2) prolonged or multiple event(s) lasting from *c.* 437 to *c.* 423 Ma.

None of the above-mentioned ages can yet be unequivocally linked directly to UHP

1
2
3
4
5
6
7
8
9
10
11
12
13
14
15
16
17
18
19
20
21
22
23
24
25
26
27
28
29
30
31
32
33
34
35
36
37
38
39
40
41
42
43
44
45
46
47
48
49
50
51
52
53
54
55
56
57
58
59
60

metamorphism; they instead could represent P-T excursions related to episodes of partial melting, each most likely following an episode of UHP metamorphism.

(3) The youngest obtained metamorphic zircon dates, scattering from *c.* 415 to *c.* 397 Ma suggest a metamorphic overprint subsequent to the previous events, likely related to the exhumation following final stages of the Scandian phase of the Baltica-Laurentia collision, first of all by translation toward the foreland, then by motion on major west-vergent detachments, but both relating to exhumation of Scandian UHP rocks.

(4) Multiple zircon growth events recorded in the Fjærtøft gneiss reflect its complicated and protracted metamorphic evolution. It is inferred that such complex metamorphic zircon ages pattern resulted from several subduction-exhumation cycles, as predicted by the dunk tectonics model for the Scandinavian Caledonides.

(5) The data **are consistent with predictions** of the dunk tectonics model, indicating that it provides a plausible explanation for the development of a major part of the Scandinavian Caledonides.

Acknowledgements

We thank Melanie Schmitt for her assistance with the laser ablation analysis. Hannes Brueckner and David Young are acknowledged for their helpful reviews. KW, SC and JM were supported by the National Science Centre (Poland) CALSUB project no. 2014/14/E/ST10/00321. This is Vegacenter publication **#016**.

Declaration of Interest

None

664

665 **References**

666 Andersen, T. B., Jamtveit, B., Dewey, J. F. & Swensson, E. 1991. Subduction and
667 eduction of continental crust: major mechanisms during continent–continent collision and
668 orogenic extensional collapse, a model based on the south Norwegian Caledonides. *Terra*
669 *Nova* **3**, 303–310. <http://dx.doi.org/10.1111/j.1365-3121.1991.tb00148.x>.

670

671 Barnes, C., Majka, J., Schneider, D. A., Walczak, K., Bukala, M. & Kościńska, K.,
672 2019. High-spatial resolution dating of zircon and monazite reveals late Cambrian
673 subduction of the Vaimok Lens of the Seve Nappe Complex in the Scandinavian
674 Caledonides of Sweden, *Contributions to Mineralogy and Petrology*, in press,
675 <https://doi.org/10.1007/s00410-018-1539-1>.

676

677 Bingen, O. & van Breemen, O. 1998. Tectonic regimes and terrane boundaries in the high
678 grade Sveconorwegian belt of SW Norway, inferred from U-Pb zircon geochronology
679 and geochemical signature of augen gneiss suites. *Journal of the Geological Society*,
680 *London* **155**, 143–154.

681

682 Bingen, B., Davis, W. J. & Austrheim, H. 2001. Zircon U-Pb geochronology in the
683 Bergen arc eclogites and their Proterozoic protoliths, and implications for the pre-
684 Scandian evolution of the Caledonides in western Norway, *Geological Society of*
685 *America Bulletin* **113**, 640–649.

686

1
2
3
4
5
6
7
8
9
10
11
12
13
14
15
16
17
18
19
20
21
22
23
24
25
26
27
28
29
30
31
32
33
34
35
36
37
38
39
40
41
42
43
44
45
46
47
48
49
50
51
52
53
54
55
56
57
58
59
60

Bingen, B. & Solli, A. 2009. Geochronology of magmatism in the Caledonian and Sveconorwegian belts of Baltica: synopsis for detrital zircon provenance studies. *Norwegian Journal of Geology* **89**, 267-290

Black, L. P., Kamo, S. L. , Allen, C. M., Davis, D. W., Aleinikoff, J. N., Valley, J. W., Mundil, R., Campbell, I. H., Korsch, R. J., Williams, I. S. & Foudoulis, C. 2004. Improved $^{206}\text{Pb}/^{238}\text{U}$ microprobe geochronology by the monitoring of a trace-element-related matrix effect; SHRIMP, ID-TIMS, ELA-ICP-MS and oxygen isotope documentation for a series of zircon standards, *Chemical Geology* **205** (1–2), 115–140.

Bröcker, M., Klemm, R., Kooijman, E., Berndt, J. & Larinov, A. 2010. Zircon geochronology and trace element characteristics of eclogites and granulites from the Orlica-Śnieżnik complex, Bohemian Massif. *Geological Magazine* **147**, 339–362.

Brueckner, H.K., 2006. Dunk, dunkless and re-dunk tectonics: a model for metamorphism, lack of metamorphism, and repeated metamorphism of HP/UHP terranes. *International Geology Review* **48**/11, 978-995.

Brueckner, H. K., Carswell, D. A., Griffin, W. L., Medaris L. G. Jr., Van Roermund, H. L. M., & Cuthbert, S. J. 2010. The mantle and crustal evolution of two garnet peridotite suites from the Western Gneiss Region, Norwegian Caledonides: An isotopic investigation. *Lithos* **117**, 1–19.

710

711 Brueckner, H. K. & van Roermund, H. L. M. 2004. Dunk tectonics: a multiple
712 subduction/ eduction model for the evolution of the Scandinavian Caledonides. *Tectonics*
713 **23**, TC2004, [doi:10.1029/2003TC001502](https://doi.org/10.1029/2003TC001502).

714

715 Brueckner, H. K., van Roermund, H. L. M. & Pearson, N. J. 2004. An Archean(?) to
716 Paleozoic evolution for garnet peridotite lens with sub-Baltic Shield affinity within the
717 Seve Nappe Complex of Jämtland, Sweden, Central Scandinavian Caledonides. *Journal*
718 *of Petrology* **45** (2), 415–437. <https://doi.org/10.1093/petrology/egg088>

719

720 Brueckner, H. K. & van Roermund, H. L. M. 2007. Concurrent HP metamorphism on
721 both margins of Iapetus: Ordovician ages for eclogites and garnet pyroxenites from the
722 Seve Nappe Complex, Swedish Caledonides. *Journal of the Geological Society, London*
723 **164**, 117–128.

724

725 Brueckner, H. K. & Cuthbert, S. J. 2013. Extension, disruption, and translation of an
726 orogenic wedge by exhumation of large ultrahigh-pressure terranes: Examples from the
727 Norwegian Caledonides. *Lithosphere* **5** (3), 277–289.

728

729 Bułała, M., Klonowska, I., Barnes, C., Majka, J., Kościńska, K., Janák, M., Fassmer, K.,
730 Broman, C. & Luptáková, J. 2018. UHP metamorphism recorded by phengite eclogite
731 from the Caledonides of northern Sweden: P–T path and tectonic implications. *Journal of*
732 *Metamorphic Geology* **36**, 529–545 <https://doi.org/10.1111/jmg.12306>.

1
2
3 733
4
5 734 Butler, J. P., Jamieson, R. A. Steenkamp, H. M. & Robinson, P. 2013. Discovery of
6
7 735 coesite–eclogite from the Nordøyane UHP domain, Western Gneiss Region, Norway:
8
9 736 field relations, metamorphic history, and tectonic significance. *Journal of Metamorphic*
10
11 737 *Geology* **31**, 147–163.
12
13
14 738
15
16 739 Carswell, D. A. & van Roermund H. L .M. 2005. On multi-phase mineral inclusions
17
18 740 associated with microdiamond formation in mantle-derived peridotite lens at Bardane on
19
20 741 Fjærtøft, west Norway. *European Journal of Mineralogy* **17**, 31–42.
21
22
23 742
24
25 743 Carswell, D. A., Van Roermund, H. L. M. & Wiggers Devries, D. F. 2006. Scandian
26
27 744 Ultrahigh-Pressure Metamorphism of Proterozoic Basement Rocks on Fjærtøft and Otrøy,
28
29 745 Western Gneiss Region, Norway. *International Geology Review* **48**, 957–977.
30
31
32 746
33
34 747 Cawood, P.A., Strachan, R., Cutts, K., Kinny, P.D., Hand, M. & Pisarevsky, S. 2010.
35
36 748 Neoproterozoic orogeny along the margin of Rodinia: Valhalla orogen, North Atlantic.
37
38 749 *Geology* **38**, 99–102.
39
40
41 750
42
43 751 Corfu, F. & Andersen, T. B. 2002. U-Pb ages of the Dalsfjord complex, SW Norway, and
44
45 752 their bearing on the correlation of allochthonous crystalline segments of the Scandinavian
46
47 753 Caledonides: *International Journal of Earth Sciences* **91**, p. 955–963,
48
49 754 doi:10.1007/s00531-002-0298-3.
50
51
52
53 755
54
55
56
57
58
59
60

- 756 Cuthbert, S. J., Harvey, M. A. & Carswell, D. A. 1983. A tectonic model for the
757 metamorphic evolution of the Basal Gneiss Complex, western South Norway: *Journal of*
758 *Metamorphic Geology* **1**, p. 63–90, doi:10.1111/j.1525-1314.1983.tb00265.x.
- 759
- 760 Cuthbert, S. J., Carswell, D. A., Krogh-Ravna, E. J. & Wain, A. 2000. Eclogites and
761 eclogites in the Western Gneiss Region, Norwegian Caledonides. *Lithos* **52**, 165–195.
762 [http://dx.doi.org/10.1016/S0024-4937\(99\)00090-0](http://dx.doi.org/10.1016/S0024-4937(99)00090-0).
- 763
- 764 Cutts, J.A. & Smit, M.A. 2018, Rates of deep continental burial from Lu-Hf garnet
765 chronology and Zr-in-rutile thermometry on (ultra-)high pressure rocks. *Tectonics* **37**, 71-
766 88 doi: 10.1002/2017TC004723.
- 767
- 768 DesOrmeau, J. W., Gordon, S. M., Kylander-Clark, A. R. C., Hacker, B. R., Bowring, S.
769 A., Schoene, B. & Samperton, K. M. 2015. Insights into (U)HP metamorphism of the
770 Western Gneiss Region, Norway: a high-spatial resolution and high-precision zircon
771 study. *Chemical Geology* **414**, 138–155.
- 772
- 773 Dobrzhinetskaya, L., Eide, E. A., Larsen, R. B., Sturt, B. A., Trønnes, R. G., Smith, D.
774 C., Taylor, W. R. & Posukhova, T. V. 1995. Microdiamond in high-grade metamorphic
775 rocks of the Western Gneiss Region, Norway: *Geology* **23**, p. 597–600.
- 776
- 777 Emmett, T. 1996. The provenance of pre-Scandian continental flakes within the
778 Caledonide orogen of south-central Norway, in *Precambrian Crustal Evolution in the*

- 779 *North Atlantic Region* (Brewer, T. S., ed.), pp. 359-366. Geological Society of London
780 Special Publication no. 112.
781
782 Fassmer, K., Klonowska, I., Walczak, K., Andersson, B., Froitzheim, N., Majka, J.,
783 Fonseca, R. O. C., Münker, C., Janák, M. & Whitehouse, M. 2017. Middle Ordovician
784 subduction of continental crust in the Scandinavian Caledonides: an example from
785 Tjeliken, Seve Nappe Complex, Sweden. *Contribution to Mineralogy and Petrology* **172**,
786 103, <https://doi.org/10.1007/s00410-017-1420-7>.
787
788 Gaál, G. & Gorbastshev, R. 1991. An Outline of the precambrian evolution of the baltic
789 shield. *Precambrian Research* **35**, 15-52.
790
791 Gee, D.G. 1980. Basement–cover relationships in the central Scandinavian Caledonides.
792 *Geologiska Föreningens i Stockholm Förhandlingar* **102**, p. 455–474,
793 <https://doi.org/10.1080/11035898009454500>.
794
795 Gee, D. G., Juhlin, C., Pascal, C. & Robinson, P. 2010. Collisional Orogeny in the
796 Scandinavian Caledonides (COSC). *Geologiska Föreningens i Stockholm Förhandlingar*
797 **132**, 29–44.
798
799 Gee, D. G., Janák, M., Majka, J., Robinson, P. & van Roermund, H. 2013. Subduction
800 along and within the Baltoscandian margin during closing of the Iapetus Ocean and
801 Baltica–Laurentia collision. *Lithosphere* **5**, 169–178.

802

803 Gee, D. G., Ladenberger, A., Dahlqvist, P., Majka, J., Be'eri-Shlevin, Y., Frei, D. &
804 Thomsen, T. 2014. The Baltoscandian margin detrital zircon signatures of the central
805 Scandes. In: *New Perspectives on the Caledonides of Scandinavia and Related Areas* (eds
806 Corfu, F., Gasser, D. & Chew, D. M.), pp. 131–155. Geological Society, London, Special
807 Publications no. 390.

808

809 Gee, D. G., Andréasson, P.-G., Lorenz, H., Frei, D. & Majka, J. 2015. Detrital zircon
810 signatures of the Baltoscandian margin along the Arctic Circle Caledonides in Sweden:
811 The Sveconorwegian connection. *Precambrian Research* **256**, 40-56.

812

813 Gordon, S. M., Whitney, D. L., Teyssier, C., Fossen, H. & Kylander-Clark, A. R. C.
814 2016. Geochronology and geochemistry of zircon from the northern Western Gneiss
815 Region: Insights into the Caledonian tectonic history of western Norway. *Lithos* **246-247**,
816 134-148.

817

818 Griffin, W. L. & Brueckner, H. K. 1985. REE, Rb–Sr and Sm–Nd studies of Norwegian
819 eclogites. *Chemical Geology* **52**, 249–271. [http://dx.doi.org/10.1016/0168-](http://dx.doi.org/10.1016/0168-9622(85)90021-1)
820 [9622\(85\)90021-1](http://dx.doi.org/10.1016/0168-9622(85)90021-1).

821

822 Grimmer, J. C., Glodny, J., Drüppel, K., Greiling, R. O. & Kontny, A. 2015. Early- to
823 mid-Silurian extrusion wedge tectonics in the central Scandinavian Caledonides. *Geology*
824 **43**, 347–350.

1
2
3
4
5
6
7
8
9
10
11
12
13
14
15
16
17
18
19
20
21
22
23
24
25
26
27
28
29
30
31
32
33
34
35
36
37
38
39
40
41
42
43
44
45
46
47
48
49
50
51
52
53
54
55
56
57
58
59
60

825

826 Hacker, B. R. & Gans, P. B. 2005. Continental collisions and the creation of ultrahigh-

827 pressure terranes: petrology and thermochronology of nappes in the central Scandinavian

828 Caledonides. *Geological Society of America Bulletin* **117**, 117–134.

829 <http://dx.doi.org/10.1130/B25549.1>.

830

831 Hacker, B. R., Andersen, T. B., Johnston, S., Kylander-Clark, A. R. C., Peterman, E. M.,

832 Walsh, E. O. & Young, D. 2010. High-temperature deformation during continental-

833 margin subduction and exhumation: the ultrahigh-pressure Western Gneiss Region of

834 Norway. *Tectonophysics* **480** (1–4), 149–171.

835 <http://dx.doi.org/10.1016/j.tecto.2009.08.012>.

836

837 Hacker, B. R., Kylander-Clark, A. R. C., Holder, R., Andersen, T. B., Peterman, E. M.,

838 Walsh, E. O. & Munnikhuis, J. K. 2015. Monazite response to ultrahigh-pressure

839 subduction from U–Pb dating of laser ablation split stream. *Chemical Geology* **409**, 28–

840 41.

841

842 Holder, R. M., Hacker, B. R., Kylander-Clark, A. R. C. & Cottle, J. M. 2015. Monazite

843 trace-element and isotopic signatures of (ultra)high-pressure metamorphism: examples

844 from the Western Gneiss Region, Norway. *Chemical Geology* **409**, 99–111.

845

- 846 Jackson, S.E., Pearson, N.J., Griffin, W.L. & Belousova, E.A. 2004. The application of
847 laser ablation-inductively coupled plasma-mass spectrometry to in situ U-Pb zircon
848 geochronology. *Chemical Geology* **211**, 47–69.
- 849
- 850 Jamtveit, B., Carswell, D.A. & Mearns, E.W. 1991. Chronology of the high-pressure
851 metamorphism of Norwegian garnet peridotites/pyroxenites. *Journal of Metamorphic*
852 *Geology* **9**, 125-139.
- 853
- 854 Janák, M., van Roermund, H., Majka, J. & Gee, D. 2013. UHP metamorphism recorded
855 by kyanite-bearing eclogite in the Seve Nappe Complex of northern Jämtland, Swedish
856 Caledonides. *Gondwana Research* **23**, 865-879.
- 857
- 858 Kirkland, C. L., Daly, J. S. & Whitehouse, M. J. 2006. Granitic magmatism of
859 Grenvillian and late Neoproterozoic age in Finnmark, Arctic Norway—Constraining pre-
860 Scandian deformation in the Kalak Nappe Complex. *Precambrian Research* **145**, 24–52.
- 861
- 862 Klonowska, I., Janák, M., Majka, J., Froitzheim, N. & Kościńska, K. 2016. Eclogite and
863 garnet pyroxenite from Stor Jougdan, Seve Nappe Complex, Sweden: implications for
864 UHP metamorphism of allochthons in the Scandinavian Caledonides. *Journal of*
865 *Metamorphic Geology* **34**, 103–119.
- 866
- 867 Klonowska, I., Majka, J., Janak, M., Gee, D.G. & Ladenberger, A. 2014. Pressure –
868 temperature evolution of a kyanite – garnet polytic gneiss from Areskutan: evidence of

1
2
3
4
5
6
7
8
9
10
11
12
13
14
15
16
17
18
19
20
21
22
23
24
25
26
27
28
29
30
31
32
33
34
35
36
37
38
39
40
41
42
43
44
45
46
47
48
49
50
51
52
53
54
55
56
57
58
59
60

869 ultra-high-pressure metamorphism of the Seve Nappe Complex, west-central Jamtland,
870 Swedish Caledonides. In *New Perspectives on the Caledonides of Scandinavia and*
871 *Related Areas* (Corfu, F., Gasser, D. & Chew, D. M. eds), pp. 321-336. Geological
872 Society of London, Special Publications no. 390, <http://dx.doi.org/10.1144/SP390.7>.
873
874 Klonowska, I., Janák, M., Majka, J., Petrik, I., Froitzheim, N., Gee, D.G. & Sasinkowá,
875 V. 2017. Microdiamond on Åreskutan confirms regional UHP metamorphism in the Seve
876 Nappe Complex of the Scandinavian Caledonides. *Journal of Metamorphic Geology* **35**,
877 541–564.
878
879 Kooijman, E., Upadhyay, D., Mezger, K., Raith, M.M., Berndt, J. & Srikantappa, C.
880 2011. Response of the U–Pb chronometer and trace elements in zircon to ultrahigh-
881 temperature metamorphism: The Kadavur anorthosite complex, southern India. *Chemical*
882 *Geology* **290**, 177-188.
883
884 Kooijman, E., Berndt, J. & Mezger, K. 2012. U-Pb dating of zircon by laser ablation ICP-
885 MS: recent improvements and new insights. *European Journal of Mineralogy* **24** (1), 5-
886 21.
887
888 Kooijman, E., Smit, M. A., Ratschbacher, L. & Stearns, M. A. 2017. A view into crustal
889 evolution at mantle depths. *Earth and Planetary Science Letters* **465**, 59-69.

- 891 Krill, A. G. 1980. Tectonics of the Oppdal area, central Norway. *Geologiska Föreningens*
892 *i Stockholm Förhandlingar* **102**, 523–530.
- 893
- 894 Krill, A. G. 1985. Relationship between the western gneiss region and the Trondheim
895 region: Stockwerk tectonics reconsidered. In *The Caledonide Orogen – Scandinavia and*
896 *Related Areas* (Gee, D. G. & Sturt, B. A. eds) pp. 475–483. John Wiley and Sons,
897 Chichester.
- 898
- 899 Krogh, E. J. 1977. Evidence for Precambrian continent–continent collision in western
900 Norway. *Nature* **267**, 17–19. <http://dx.doi.org/10.1038/267017a0>.
- 901
- 902 Krogh, T. E., Kamo, S. L., Robinson, P., Terry, M. P. & Kwok, K. 2011. U–Pb zircon
903 geochronology of eclogites from the Scandian Orogen, northern Western Gneiss Region,
904 Norway: 14–20 million years between eclogite crystallization and return to amphibolite-
905 facies conditions. *Canadian Journal of Earth Sciences* **48**, 441–472.
906 <http://dx.doi.org/10.1139/E10-076>.
- 907
- 908 Kylander-Clark, A. R. C., Hacker, B. R. & Mattinson, J.M. 2008. Slow exhumation of
909 UHP terranes: titanite and rutile ages of the Western Gneiss Region, Norway. *Earth and*
910 *Planetary Science Letters* **272** (3–4), 531–540.
911 <http://dx.doi.org/10.1016/j.epsl.2008.05.019>.
- 912

1
2
3 913 Kylander-Clark, A. R. C., Hacker, B. R., Johnson, C. M., Beard, B. L. & Mahlen, N. J.
4
5 914 2009. Slow subduction of a thick ultrahigh-pressure terrane. *Tectonics* **28**, TC2003,
6
7 915 doi:10.1029/2007TC002251.
8
9
10 916
11
12 917 Labrousse, L., Jolivet, L., Agard, P., Hebert, R. & Andersen, T. B. 2002. Crustal-scale
13
14 918 boudinage and migmatization of gneiss during their exhumation in the UHP Province of
15
16
17 919 Western Norway. *Terra Nova* **14**, 263–270, 2002.
18
19 920
20
21 921 Ladenberger, A., Be'eri-Shlevin, Y., Claesson, S., Gee, D. G., Majka, J. & Romanova, I.
22
23 922 V. 2014. Tectonometamorphic evolution of the Åreskutan Nappe-Caledonian history
24
25 923 revealed by SIMS U–Pb zircon geochronology. In *New perspectives on the Caledonides*
26
27 924 *of Scandinavia and Related Areas* (Corfu, F., Gasser, D. & Chew, D.M. eds) pp. 337-368.
28
29 925 Geological Society of London, Special Publications no. 390.
30
31 926
32
33 927 Larsen, R. B., Eide, E. A., & Burke, A. J. 1998. Evolution of metamorphic volatiles
34
35 928 during exhumation of microdiamond-bearing granulites in the Western Gneiss Region,
36
37 929 Norway. *Contributions to Mineralogy and Petrology* **133**, 106-121.
38
39
40 930
41
42 931 Liu, P. & Massone, H.-J. 2019. An anticlockwise P-T-t path at high-pressure, high-
43
44 932 temperature conditions for a migmatitic gneiss from the island of Fjortoft, Western
45
46 933 Gneiss Region, Norway, indicates two burial events during the Caledonian orogeny.
47
48 934 *Journal of Metamorphic Geology*, <https://doi.org/10.1111/jmg.12476>.
49
50
51 935
52
53
54
55
56
57
58
59
60

1
2
3 936 Ludwig, K. R. 2012. User's Manual for Isoplot 3.75 a Geochronological Toolkit for
4
5 937 Microsoft Excel. Berkeley Geochronology Center Special Publication no. 5. Downloaded
6
7
8 938 at: http://www.bgc.org/isoplot_etc/isoplot.html 2015-02-06.
9

10 939

11
12 940 Majka, J., Be'eri-Shlevin, Y., Gee, D. G., Ladenberger, A., Claesson, S., Konecny, P. &
13
14 941 Klonowksa, I. 2012. Multiple monazite growth in the Åreskutanmigmatite: evidence for a
15
16 942 polymetamorphic Late Ordovician to Late Silurian evolution in the Seve Nappe Complex
17
18 943 of west-central Jämtland, Sweden. *Journal of Geosciences* **57**, 3–2.
19

20 944

21
22
23 945 Majka, J., Rosén, Å., Janák, M., Froitzheim, N., Klonowska, I., Manecki, M., Sasinková,
24
25 946 V. & Yoshida, K. 2014. Microdiamond discovered in the Seve Nappe (Scandinavian
26
27 947 Caledonides) and its exhumation by the “vacuum-cleaner” mechanism. *Geology* **42**,
28
29 948 1107–1110.
30

31 949

32
33
34 950 Medaris, L. G., Brueckner, H. K., Cai, Y., Griffin W. L., Janák, M. 2018. Eclogites in
35
36 951 peridotite massifs in the Western Gneiss Region, Scandinavian Caledonides: Petrogenesis
37
38 952 and comparison with those in the Variscan Moldanubian Zone. *Lithos* **322**, 352-346.
39

40 953

41
42
43 954 Mezger, K. & Krogstad, E. J. 1997. Interpretation of discordant U–Pb zircon ages: an
44
45 955 evaluation. *Journal of Metamorphic Geology* **15**, 127-140.
46
47
48

49 956
50
51
52
53
54
55
56
57
58
59
60

1
2
3
4
5
6
7
8
9
10
11
12
13
14
15
16
17
18
19
20
21
22
23
24
25
26
27
28
29
30
31
32
33
34
35
36
37
38
39
40
41
42
43
44
45
46
47
48
49
50
51
52
53
54
55
56
57
58
59
60

957 Mørk, M. B. E., Kullerød, K. V. & Stabel, A. 1988. Sm–Nd dating of Seve eclogites,
958 Norrbotten, Sweden-evidence for early Caledonian (505 Ma) subduction. *Contributions*
959 *to Mineralogy and Petrology* **99**, 344–351.

960

961 Norton, M.G. 1991. The Nordfjord-Sogn Detachment, W. Norway. *Norsk Geologisk*
962 *Tidsskrift* **67**, pp. 93-106.

963

964 Paulsson, O. & Adréasson, P. G. 2002. Attempted break-up of Rodinia at 850 Ma:
965 geochronological evidence from the Seve–Kalak Superterrane, Scandinavian
966 Caledonides. *Journal of the Geological Society, London* **159**, 751–761.

967

968 Quas-Cohen, A. 2013. Norwegian orthopyroxene eclogites: petrogenesis and implications
969 for metasomatism and crust-mantle interactions during subduction of continental crust.
970 Unpublished PhD thesis, University of Manchester.

971

972 Roberts, R. J., Corfu, F., Torskvik, T. H., Hetherington, C. J. & Ashwal, L. D. 2010. Age
973 of alkaline rocks in the Seiland Igneous Province, Northern Norway. *Journal of the*
974 *Geological Society, London* **167**, 71-81.

975

976 Robinson, P. 1995. Extension of Trollheimen tectonostratigraphic sequence in deep
977 synclines near Molde and Brattvåg, Western Gneiss Region, southern Norway. *Norsk*
978 *Geologisk Tidsskrift* **75**, 181–197.

979

- 980 Robinson, P, Langenhorst, F. & Terry, M. P. 2003. Interpretation of inclusions in
981 kyanite-garnet gneiss: Fjortoft, Western Norway. Alice Wain Eclogite Field Symposium,
982 Selje, West Norway. Abstract Volume, Norges geologiske undersøkelse Report No.
983 2003.055, 119-120.
- 984
- 985 Robinson, P. & Hollocher, K. 2008. Geology of Trollheimen. In: Robinson, P., Roberts,
986 D., Gee, D. G. (Eds.), Guidebook: a tectonostratigraphic transect across the central
987 Scandinavian Caledonides. NGU report 2008.064, pt. II. Geological Survey of Norway,
988 Trondheim, pp. 6-1–6-7.
- 989
- 990 Robinson, P., Roberts, D., Gee, D. G. & Solli, A. 2014. A major synmetamorphic Early
991 Devonian thrust and extensional fault system in the mid-Norway Caledonides: relevance
992 to exhumation of HP and UHP rocks. In *New Perspectives on the Caledonides of*
993 *Scandinavia and Related Areas* (Corfu, F., Gasser, D. & Chew, D. M. eds) pp. 241-270.
994 Geological Society of London, Special Publications no. 390.
- 995
- 996 Røhr, T. S., Corfu, F., Austrheim, H. & Andersen, T. B. 2004. Sveconorwegian U-Pb
997 zircon and monazite ages of granulite-facies rocks, Hisarøya, Gulen, Western Gneiss
998 Region, Norway. *Norwegian Journal of Geology* **84**, 251-256.
- 999
- 1000 Root, D. B., Hacker, B. R., Gans, P. B., Ducea, M. N., Eide, E. A. & Mosenfelder, L.
1001 2005. Discrete ultrahigh-pressure domains in the Western Gneiss Region, Norway:

1
2
3 1002 Implications for formation and exhumation. *Journal of Metamorphic Geology* **23**, (1), p.
4
5 1003 45–61, doi:10.1111/j.1525-1314.2005.00561.x.
6
7 1004
8
9
10 1005 Root, D. & Corfu, F. 2012. U–Pb geochronology of two discrete Ordovician high-
11
12 1006 pressure metamorphic events in the Seve Nappe Complex, Scandinavian Caledonides.
13
14 1007 *Contributions to Mineralogy and Petrology* **163**, 769–788.
15
16 1008
17
18
19 1009 Scambelluri M., van Roermund H. L. M. & Pettke T. 2010. Mantle wedge peridotites:
20
21 1010 Fossil reservoirs of deep subduction zone processes: Inferences from high and ultrahigh-
22
23 1011 pressure rocks from Bardane (Western Norway) and Ulten (Italian Alps). *Lithos* **120**,
24
25 1012 186-201.
26
27
28 1013
29
30
31 1014 Sláma J., Košler J., Condon D. J., Crowley J. L., Gerdes A., Hanchar J. M., Horstwood
32
33 1015 M. S. A., Morris G. A., Nasdala L., Norberg N., Schaltegger U., Schoene B., Tubrett M.
34
35 1016 N. & Whitehouse M. J. 2008. Plešovice zircon — A new natural reference material for
36
37 1017 U–Pb and Hf isotopic microanalysis. *Chemical Geology* **249**, 1-35.
38
39 1018
40
41
42 1019 Smit, M. A., Scherer, E. E., Bröcker, M. & van Roermund, H. L. M. 2010, Timing of
43
44 1020 eclogite facies metamorphism in the southernmost Scandinavian Caledonides by Lu–Hf
45
46 1021 and Sm–Nd geochronology. *Contributions to Mineralogy and Petrology* **159**, 521-539.
47
48 1022
49
50
51 1023 Smit, M. A., Bröcker, M., Kooijman, E., & Scherer, E. E. 2011. Provenance and
52
53 1024 exhumation of an exotic eclogite-bearing nappe in the Caledonides: a U–Pb and Rb–Sr
54
55
56
57
58
59
60

- 1025 study of the Jæren nappe, SW Norway. *Journal of the Geological Society London* **168**,
1026 421-439.
- 1027
- 1028 Stephens, M. B. & Gee, D. G. 1985. A tectonic model for the evolution of the eugeoclinal
1029 terranes in the central Scandinavian Caledonides. In *The Caledonide Orogen—*
1030 *Scandinavia and Related Areas*, (eds D. G. Gee & G. A. Sturt), pp. 953 – 978, John
1031 Wiley, Hoboken, N.J.
- 1032
- 1033 Stephens, M. 1988. The Scandinavian Caledonides; a complexity of collisions. *Geology*
1034 *Today* **4**, 20–24.
- 1035
- 1036 Stephens, M. B. & Gee, D. G. 1989. Terranes and polyphase accretionary history in the
1037 Scandinavian Caledonides, in *Terranes in the Circum-Atlantic Paleozoic Orogens* (ed R.
1038 D. Dallmeyer) pp. 17-30, Geological Society of America, Special Papers no. 230.
- 1039
- 1040 Terry, M. P., Robinson P., Hamilton, M. A. & Jercinovic, M. J. 2000. Monazite
1041 geochronology of UHP and HP metamorphism, deformation and exhumation,
1042 Nordøyane, Western Gneiss Region, Norway, *American Mineralogist* **85**, 1651 – 1664.
- 1043
- 1044 Terry, M. P., Robinson, P. & Ravna, E. J. K. 2000. Kyanite eclogite thermobarometry
1045 and evidence for thrusting of UHP over HP metamorphic rocks, Nordøyane, Western
1046 Gneiss Region, Norway. *American Mineralogist* **85**, 1637–1650.
- 1047

1
2
3
4
5
6
7
8
9
10
11
12
13
14
15
16
17
18
19
20
21
22
23
24
25
26
27
28
29
30
31
32
33
34
35
36
37
38
39
40
41
42
43
44
45
46
47
48
49
50
51
52
53
54
55
56
57
58
59
60

1048 Terry, M. P. & Robinson, P. 2004. Geometry of eclogite facies structural features;
1049 implications for production and exhumation of ultrahigh-pressure and high-pressure
1050 rocks, Western Gneiss region, Norway. *Tectonics* **23**, 1–23.

1051

1052 Tucker, R. D., Boyd, R. & Barnes, S.-J. 1990. A U–Pb zircon age for the Råna intrusion,
1053 N. Norway: New evidence of basic magmatism in the Scandinavian Caledonides in Early
1054 Silurian time. *Norsk Geologisk Tidsskrift* **70**, 229–239.

1055

1056 Tucker, R. D., Krogh, T. E. & Råheim, A. 1991. Proterozoic evolution and age-province
1057 boundaries in the central parts of the Western Gneiss Region, Norway: Results of U-Pb
1058 dating of accessory minerals from Trondheimsfjord to Geiranger, in *Mid-Proterozoic*
1059 *Laurentia-Baltica*, edited by C. F. Gower, T. Rivers, and B. Ryan, The Geological
1060 Association of Canada Special Papers, **38**, 149 – 173.

1061

1062 Tucker, R. D., Robinson, P., Solli, A., Gee, D. G., Thorsnes, T., Krogh, T. E., Nordgulen,
1063 Ø. & Bickford, M.E. 2004. Thrusting and extension in the Scandian hinterland, Norway:
1064 New U–Pb ages and tectonostratigraphic evidence. *American Journal of Science* **304** (6),
1065 477–532. <http://dx.doi.org/10.2475/ajs.304.6.477>.

1066

1067 Vrijmoed, J., Van Roermund, H. & Davies, G. 2006. Evidence for diamond-grade ultra-
1068 high pressure metamorphism and fluid interaction in the Svartberget Fe–Ti garnet
1069 peridotite–websterite body, Western Gneiss Region, Norway. *Mineralogy and Petrology*
1070 **88**, 381-405.

- 1071
- 1072 Vrijmoed, J. C., Austrheim, H., John, T., Hin, R. C., Corfu, F. & Davies, G. R. 2013.
- 1073 Metasomatism in the ultrahigh-pressure Svartberget garnet-peridotite (Western Gneiss
- 1074 Region, Norway): Implications for the transport of crust-derived fluids within the mantle.
- 1075 *Journal of Petrology* **54**, 1815-1848.
- 1076
- 1077 Walker, S., Thirlwall, M. F., Strachan, R. A. & Bird, A. F. 2016. Evidence from Rb–Sr
- 1078 mineral ages for multiple orogenic events in the Caledonides of Shetland, Scotland.
- 1079 *Journal of the Geological Society* **173**, 489–503.
- 1080
- 1081 Walsh, E. O., Hacker, B. R., Gans, P. B., Grove, M. & Gehrels, G. 2007. Protolith ages
- 1082 and exhumation histories of (ultra)high-pressure rocks across the Western Gneiss Region,
- 1083 Norway. *Journal of Metamorphic Geology* **119**, 289–301.
- 1084
- 1085 Walsh, E. O., Hacker, B. R., Gans, P. B., Wong, M. S. & Andersen, T. B. 2013. Crustal
- 1086 exhumation of the Western Gneiss Region UHP terrane, Norway: $^{40}\text{Ar}/^{39}\text{Ar}$
- 1087 thermochronology and fault-slip analysis. *Tectonophysics* **608**, 1159–1179.
- 1088
- 1089 Wiedenbeck, M., Allé, P., Corfu, F., Griffin, W. L., Meier, M., Oberli, F., von Quadt, A.,
- 1090 Roddick, J.C. & Spiegel, W. 1995. Three natural zircon standards for U–Th–Pb, Lu–Hf,
- 1091 trace element and REE analyses. *Geostandards Newsletter* **19**, 1–23.
- 1092

1
2
3 1093 Wilks, W. & Cuthbert, S. J. 1994. The evolution of the Hornelen Basin detachment
4
5 1094 system, western Norway: Implications for the style of late orogenic extension in the
6
7 1095 southern Scandinavian Caledonides. *Tectonophysics* **238**, 1-30.
8
9
10 1096
11
12
13 1097 Yakymchuk, C. & Brown, M. 2014. Behaviour of zircon and monazite during crustal
14
15 1098 melting. *Journal of the Geological Society London* **171**, 465-479.
16
17 1099
18
19
20 1100 Young, D. J. 2018. Structure of the (ultra)high-pressure Western Gneiss Region, Norway:
21
22 1101 Imbrication during Caledonian continental margin subduction. *GSA Bulletin* **130**, 926–94.
23
24 1102
25
26
27 1103 **Figure captions**
28
29 1104 Figure 1. (Colour online) (a) Simplified geological map of the Western Gneiss Region
30
31 1105 (modified after Brueckner & Cuthbert, 2013) with (b) generalised geological map of
32
33 1106 Fjortoft (after Carswell & van Roermund, 2005) showing the location of the diamond-
34
35 1107 bearing garnet kyanite gneiss. NSD - Nordfjord-Sogn detachment zone, MTD - Møre
36
37 1108 Trondelag detachment zone, black dashed line - early E/SE late W/NW décollements,
38
39 1109 black thin lines - W/NW vergent lineation directions.
40
41
42 1110
43
44
45 1111 Figure 2. (Colour online) Hand specimen of the diamond-bearing garnet-kyanite gneiss
46
47 1112 from Fjortoft (sample ID: Fj-19).
48
49 1113
50
51
52
53
54
55
56
57
58
59
60

1114 Figure 3. (Colour online) Cathodoluminescence images of representative zircon crystals
1115 from the Fjortoft diamond-bearing garnet kyanite gneiss. White circles mark analytical
1116 spots and given numbers indicate ^{206}Pb - ^{238}U dates.

1117

1118 Figure 4. (Colour online) (a-d) U-Pb concordia diagram for zircon analyses; (a) all
1119 analyses for both metamorphic and detrital zircon domains, (b) concordia diagram of
1120 zircon with Caledonian ages with inset (c) showing ages for which Concordia age has
1121 been calculated. (d) Magnification of the fragment of Concordia diagram (a) showing late
1122 Precambrian dates. (e) Histogram of ^{206}Pb - ^{238}U age frequency of metamorphic zircon
1123 domains. (f) Histogram of ^{207}Pb - ^{206}Pb age frequency of concordant detrital zircon (10%
1124 discordance accepted).

1125

1126 Table 1. Summary of the U-Pb zircon analyses from the diamond-bearing garnet kyanite gneiss.

Analysis	U conc.	Ratios							Common Pb		Degree of con- cordance (%)	Ages (Ma)						Comments
		²⁰⁷ Pb/ ²⁰⁶ Pb	±2σ	²⁰⁷ Pb/ ²³⁵ U	±2σ	²⁰⁶ Pb/ ²³⁸ U	±2σ	rho:	²⁰⁶ Pb/ ²⁰⁴ Pb	f ²⁰⁶ %		²⁰⁶ Pb/ ²³⁸ U	±2σ	²⁰⁷ Pb/ ²³⁵ U	±2σ	²⁰⁷ Pb/ ²⁰⁶ Pb	±2σ	
nr	(ppm)																	
2	236	0.0558	0.0004	0.5454	0.0048	0.0709	0.0004	0.69	146049	0.01	99.6	441.7	2.6	442.0	3.2	443	14	rim
6	286	0.0554	0.0004	0.5195	0.0047	0.0680	0.0004	0.71	6482	0.27	98.8	424.0	2.6	424.8	3.1	429	14	metamorphic (no core)
17	384	0.0560	0.0003	0.5538	0.0056	0.0717	0.0006	0.79			98.7	446.5	3.5	447.5	3.7	452	14	rim
22	35	0.0555	0.0006	0.5348	0.0074	0.0699	0.0006	0.58	688	2.37	101.2	435.8	3.4	435.0	4.9	431	25	core
23	549	0.0553	0.0002	0.5219	0.0040	0.0685	0.0004	0.81	12869	0.13	100.6	426.8	2.6	426.4	2.7	424	10	rim
24	387	0.0552	0.0003	0.5191	0.0043	0.0682	0.0005	0.82	7163	0.23	101.1	425.3	2.8	424.6	2.9	421	11	core
25	106	0.0557	0.0004	0.5339	0.0049	0.0695	0.0004	0.69	2278	0.72	98.6	433.4	2.7	434.4	3.3	440	15	rim
27	125	0.0553	0.0004	0.5499	0.0051	0.0721	0.0005	0.72	26178	0.06	105.6	448.8	2.9	445.0	3.3	425	14	rim
28	30	0.0555	0.0008	0.5517	0.0089	0.0721	0.0005	0.47	2025	0.81	103.5	448.6	3.3	446.1	5.8	434	32	rim
30	233	0.0550	0.0003	0.5154	0.0042	0.0679	0.0004	0.74	2733	0.60	102.3	423.5	2.5	422.1	2.8	414	12	rim
31	207	0.0554	0.0002	0.5473	0.0054	0.0717	0.0006	0.89	22998	0.08	104.4	446.2	3.8	443.2	3.6	428	10	metamorphic (no core)
36	197	0.0553	0.0002	0.5332	0.0050	0.0699	0.0006	0.88	20051	0.09	102.8	435.8	3.4	433.9	3.3	424	10	metamorphic (no core)
37	211	0.0552	0.0002	0.5299	0.0048	0.0696	0.0006	0.90	6968	0.25	103.4	434.0	3.4	431.8	3.2	420	9	fragment of zircon grain
46	87	0.0562	0.0004	0.5574	0.0051	0.0719	0.0003	0.50			97.2	447.7	2.0	449.8	3.3	461	17	rim
52	307	0.0544	0.0003	0.4764	0.0036	0.0635	0.0003	0.55	356385	0.00	102.5	397.0	1.6	395.6	2.5	387	14	metamorphic (no core)
53	863	0.0553	0.0003	0.5192	0.0038	0.0681	0.0003	0.63			100.6	425.0	1.9	424.6	2.6	423	13	metamorphic (no core)
54	185	0.0561	0.0005	0.5540	0.0050	0.0716	0.0003	0.44			97.5	445.7	1.7	447.6	3.3	457	18	rim
55	839	0.0557	0.0004	0.5257	0.0061	0.0685	0.0006	0.81			97.1	427.0	3.9	429.0	4.0	440	15	core
61	182	0.0553	0.0002	0.5260	0.0044	0.0689	0.0005	0.87			100.8	429.7	3.0	429.2	2.9	426	9	metamorphic (no core)
62	265	0.0554	0.0002	0.5265	0.0031	0.0689	0.0003	0.83	15572	0.11	100.5	429.8	2.1	429.5	2.1	428	7	metamorphic (no core)
63	535	0.0553	0.0003	0.5171	0.0040	0.0678	0.0003	0.65	11250	0.16	99.4	422.8	2.1	423.2	2.7	425	13	fragment of zircon grain
64	189	0.0553	0.0002	0.5224	0.0031	0.0685	0.0003	0.78	2626	0.59	100.4	427.0	1.9	426.7	2.1	425	8	rim
65	81	0.0558	0.0004	0.5398	0.0048	0.0702	0.0003	0.52	1133	1.56	98.8	437.5	2.0	438.3	3.2	443	17	rim
67	160	0.0545	0.0005	0.5003	0.0056	0.0666	0.0004	0.53	3638	0.49	106.4	415.7	2.4	411.9	3.8	391	21	rim
71	249	0.0553	0.0002	0.5201	0.0040	0.0682	0.0004	0.86	6196	0.29	99.8	425.1	2.7	425.2	2.6	426	9	metamorphic (no core)
74	257	0.0554	0.0003	0.5264	0.0057	0.0689	0.0007	0.91	3931	0.42	100.1	429.5	4.1	429.4	3.8	429	10	rim
75	319	0.0554	0.0002	0.5258	0.0039	0.0688	0.0005	0.91			100.2	429.2	2.8	429.0	2.6	428	7	rim
78	157	0.0557	0.0003	0.5217	0.0041	0.0679	0.0004	0.78	2216	0.80	95.9	423.5	2.5	426.3	2.7	441	11	metamorphic (no core)
81	142	0.0556	0.0004	0.5335	0.0052	0.0696	0.0005	0.67	2456	0.72	99.3	433.7	2.8	434.1	3.5	437	16	metamorphic (no core)
96	250	0.0555	0.0004	0.5270	0.0044	0.0688	0.0004	0.61			98.9	429.0	2.1	429.8	2.9	434	15	metamorphic (no core)
97	385	0.0555	0.0004	0.5307	0.0044	0.0693	0.0003	0.60			99.8	432.2	2.1	432.3	2.9	433	15	core
101	147	0.0560	0.0003	0.5355	0.0047	0.0693	0.0005	0.74	3896	0.44	95.1	431.9	2.7	435.4	3.1	454	13	rim
102	233	0.0554	0.0003	0.5182	0.0041	0.0679	0.0004	0.70	103170	0.02	99.1	423.4	2.3	423.9	2.7	427	13	core
103	62	0.0554	0.0004	0.5233	0.0043	0.0685	0.0003	0.60	3546	0.46	99.5	427.0	2.0	427.4	2.9	429	15	metamorphic (no core)
104	223	0.0554	0.0003	0.5235	0.0040	0.0686	0.0004	0.71	20895	0.34	100.4	427.7	2.4	427.5	2.7	426	11	metamorphic (no core)
105	148	0.0559	0.0004	0.5068	0.0043	0.0658	0.0003	0.60			91.8	410.7	2.0	416.3	2.9	448	15	rim
60	78	0.0579	0.0005	0.6710	0.0061	0.0841	0.0003	0.43			99.2	520.6	2.0	521.3	3.7	525	18	rim
70	1362	0.0576	0.0001	0.6715	0.0040	0.0846	0.0005	0.94			101.8	523.4	2.9	521.6	2.5	514	4	core
69	118	0.0584	0.0004	0.7072	0.0063	0.0878	0.0005	0.58			99.4	542.5	2.7	543.1	3.8	546	16	rim
1	651	0.1042	0.0052	1.3385	0.0746	0.0932	0.0024	0.45	3766030	0.00	33.8	574.3	13.9	862.6	32.4	1700	92	core
5	261	0.0899	0.0005	3.3030	0.0281	0.2444	0.0017	0.77	53281	0.03	99.0	1409.5	9.0	1415.3	7.1	1424	11	core
7	251	0.2927	0.0021	16.1291	0.1504	0.3997	0.0023	0.62	9214	0.13	63.2	2167.4	10.7	2884.5	8.9	3432	11	core
12	191	0.1783	0.0010	12.5367	0.1365	0.5099	0.0048	0.86	43533	0.04	100.7	2656.0	20.5	2645.5	10.2	2637	9	core
13	128	0.0713	0.0004	1.6293	0.0273	0.1657	0.0026	0.94	3412	0.52	102.2	988.1	14.4	981.6	10.5	967	12	rim
14	1128	0.0653	0.0003	0.9729	0.0089	0.1081	0.0008	0.81	49091	0.04	84.6	661.9	4.7	690.0	4.6	783	11	core

15	206	0.0713	0.0003	1.4834	0.0124	0.1509	0.0010	0.81			93.8	905.9	5.7	923.6	5.1	966	10	rim
16	51	0.1677	0.0012	11.2274	0.2311	0.4855	0.0093	0.93	8352	0.21	100.6	2551.0	40.5	2542.2	19.2	2535	12	core
506	201	0.0830	0.0015	0.9346	0.0211	0.0817	0.0011	0.58	9400	0.17	39.9	506.2	6.4	670.0	11.1	1269	36	core
19	145	0.0651	0.0006	1.0268	0.0207	0.1145	0.0020	0.89	1246	1.31	90.0	698.7	11.9	717.3	10.4	776	19	core
743	658	0.0847	0.0006	1.4270	0.0231	0.1222	0.0018	0.90			56.8	743.3	10.3	900.3	9.7	1308	14	core
26	726	0.0760	0.0003	1.9710	0.0202	0.1882	0.0017	0.91	34372	0.05	101.6	1111.6	9.5	1105.7	6.9	1094	9	core
29	129	0.0700	0.0006	1.3920	0.0154	0.1442	0.0011	0.67	4447	0.37	93.5	868.2	6.0	885.5	6.5	929	17	core
35	960	0.0726	0.0006	1.6851	0.0318	0.1684	0.0029	0.91	20931	0.08	100.2	1003.5	15.9	1002.9	12.0	1002	16	core
39	573	0.1552	0.0013	4.9275	0.0732	0.2303	0.0028	0.82	10407	0.17	55.6	1335.9	14.8	1807.0	12.5	2404	14	core
40	485	0.1580	0.0012	4.9258	0.0798	0.2261	0.0033	0.89	52300	0.03	54.0	1314.0	17.1	1806.7	13.7	2434	13	core
42	935	0.0883	0.0006	2.1687	0.0343	0.1781	0.0025	0.89	19352	0.09	76.0	1056.3	13.8	1171.1	11.0	1390	14	core
43	442	0.0677	0.0005	1.3162	0.0186	0.1409	0.0017	0.84	15083	0.10	98.7	849.8	9.4	852.9	8.1	861	16	rim
45	605	0.0912	0.0006	3.1539	0.0372	0.2507	0.0024	0.82	27975	0.06	99.3	1442.1	12.5	1446.0	9.1	1452	13	core
48	371	0.0652	0.0009	1.2208	0.0202	0.1357	0.0012	0.52	7296	0.24	104.9	820.4	6.6	810.1	9.2	782	30	core
50	507	0.1488	0.0015	4.5197	0.0673	0.2204	0.0024	0.74	4529	0.31	55.1	1283.7	12.9	1734.6	12.4	2332	17	core
57	330	0.2115	0.0017	17.3921	0.2252	0.5963	0.0061	0.78			103.3	3014.9	24.5	2956.7	12.4	2917	13	core
59	435	0.1326	0.0033	5.8086	0.1765	0.3178	0.0056	0.58	14261	0.10	83.4	1778.8	27.2	1947.7	26.3	2132	43	core
66	279	0.1064	0.0003	2.9824	0.0428	0.2032	0.0029	0.98	18269	0.09	68.6	1192.5	15.3	1403.2	10.9	1739	5	core
68	965	0.0725	0.0003	1.6708	0.0146	0.1672	0.0013	0.91	29862	0.06	99.7	996.7	7.3	997.5	5.6	999	8	core
73	663	0.1576	0.0018	5.2052	0.1127	0.2395	0.0044	0.85	9696	0.18	56.9	1384.0	22.8	1853.5	18.4	2431	20	core
76	191	0.1777	0.0009	10.4769	0.1101	0.4275	0.0039	0.86	9230	0.19	87.2	2294.5	17.5	2477.9	9.7	2632	9	core
77	512	0.0666	0.0003	1.2174	0.0115	0.1326	0.0011	0.84			97.2	802.5	6.0	808.6	5.3	825	11	rim
80	655	0.1319	0.0009	3.1985	0.0376	0.1758	0.0017	0.82	253587	0.01	49.2	1044.2	9.2	1456.8	9.1	2124	12	rim
84	1089	0.1395	0.0012	4.2227	0.0793	0.2195	0.0037	0.89	30084	0.06	57.6	1279.2	19.4	1678.4	15.4	2221	15	core
86	269	0.1755	0.0011	11.2620	0.0972	0.4654	0.0028	0.70			94.3	2463.2	12.4	2545.1	8.0	2611	10	rim
87	153	0.1847	0.0011	12.4118	0.1241	0.4874	0.0038	0.78	9232	0.19	94.9	2559.3	16.6	2636.1	9.4	2696	10	core
88	151	0.1921	0.0012	14.0338	0.1553	0.5298	0.0049	0.84	19746	0.09	99.3	2740.4	20.7	2752.0	10.5	2761	10	core
91	33	0.1452	0.0015	3.2180	0.0506	0.1607	0.0019	0.74			41.9	960.6	10.4	1461.5	12.2	2291	18	core
92	25	0.1828	0.0014	8.2464	0.1310	0.3272	0.0046	0.88			68.1	1824.9	22.2	2258.4	14.4	2678	13	core
94	223	0.1197	0.0022	5.7115	0.1074	0.3462	0.0014	0.21			98.2	1916.4	6.6	1933.1	16.2	1951	33	core
95	37	0.0844	0.0006	2.5112	0.0225	0.2157	0.0012	0.64			96.7	1259.3	6.6	1275.3	6.5	1302	13	fragment of zircon grain
98	39	0.0637	0.0005	1.0104	0.0122	0.1150	0.0010	0.72	5605	0.31	95.8	701.7	5.8	709.1	6.1	733	18	rim
99	113	0.0689	0.0005	1.2650	0.0124	0.1333	0.0009	0.71			90.2	806.4	5.3	830.2	5.6	894	14	core
100	166	0.0658	0.0008	1.1848	0.0166	0.1306	0.0008	0.46	3066	0.56	98.8	791.0	4.8	793.5	7.7	801	26	rim
108	54	0.1390	0.0020	2.6482	0.0522	0.1381	0.0019	0.69	6571	0.26	37.7	834.1	10.6	1314.2	14.5	2215	25	core
110	194	0.1678	0.0017	8.0060	0.0934	0.3460	0.0021	0.53	4178964	0.00	75.5	1915.5	10.2	2231.7	10.5	2536	17	core

1127

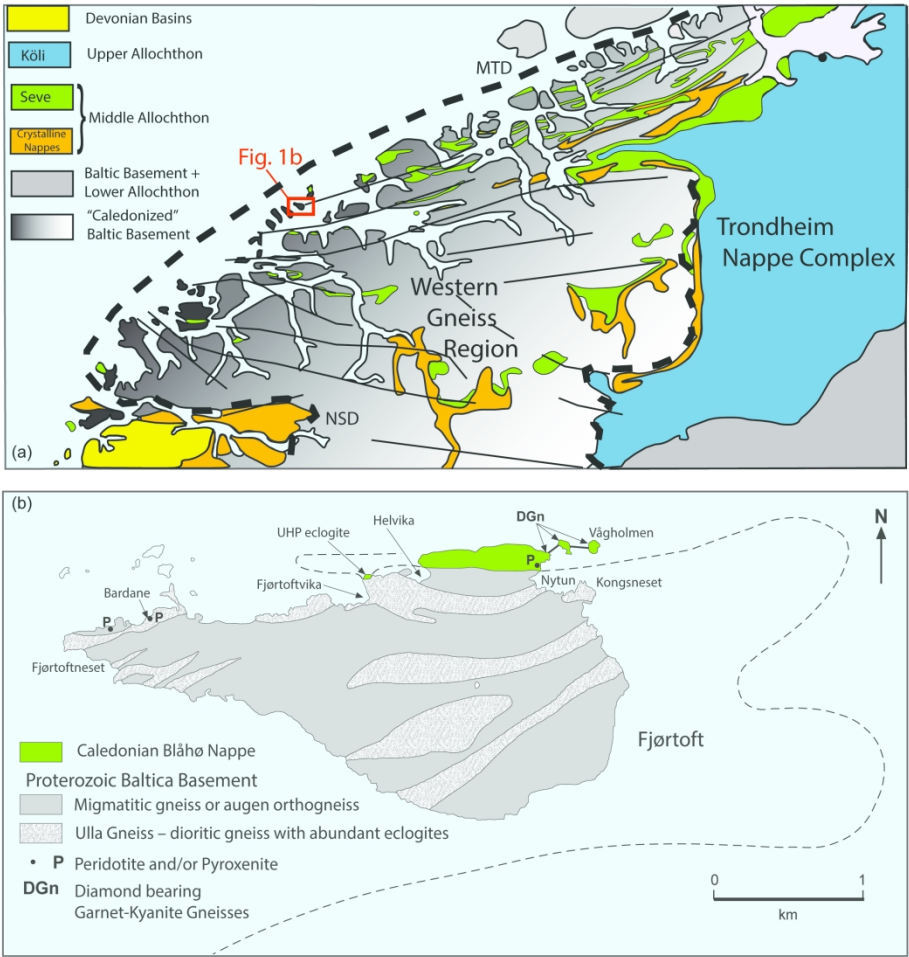


Figure 1. (Colour online) (a) Simplified geological map of the Western Gneiss Region (modified after Brueckner & Cuthbert, 2013) with (b) generalised geological map of Fjørtoft (after Carswell & van Roermund, 2005) showing the location of the diamond-bearing garnet kyanite gneiss. NSD - Nordfjord-Sogn detachment zone, MTD - Møre Trondelag detachment zone, black dashed line - early E/SE late W/NW décollements, black thin lines - W/NW vergent lineation directions.

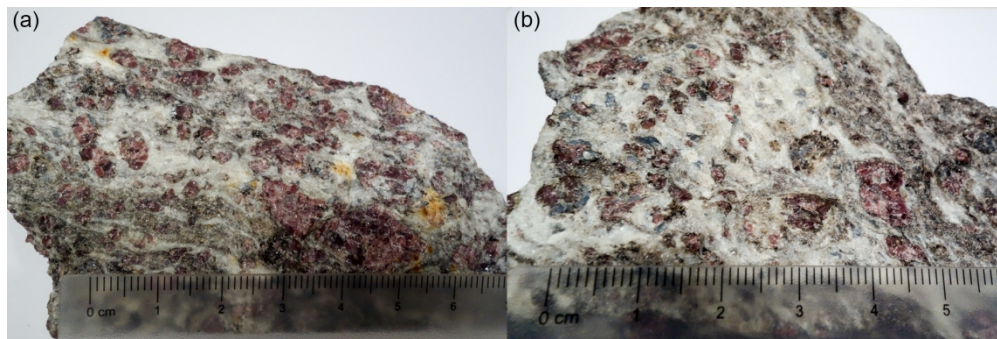


Figure 2. (Colour online) Hand specimen of the diamond-bearing garnet-kyanite gneiss from Fjørtoft (sample ID: Fj-19).

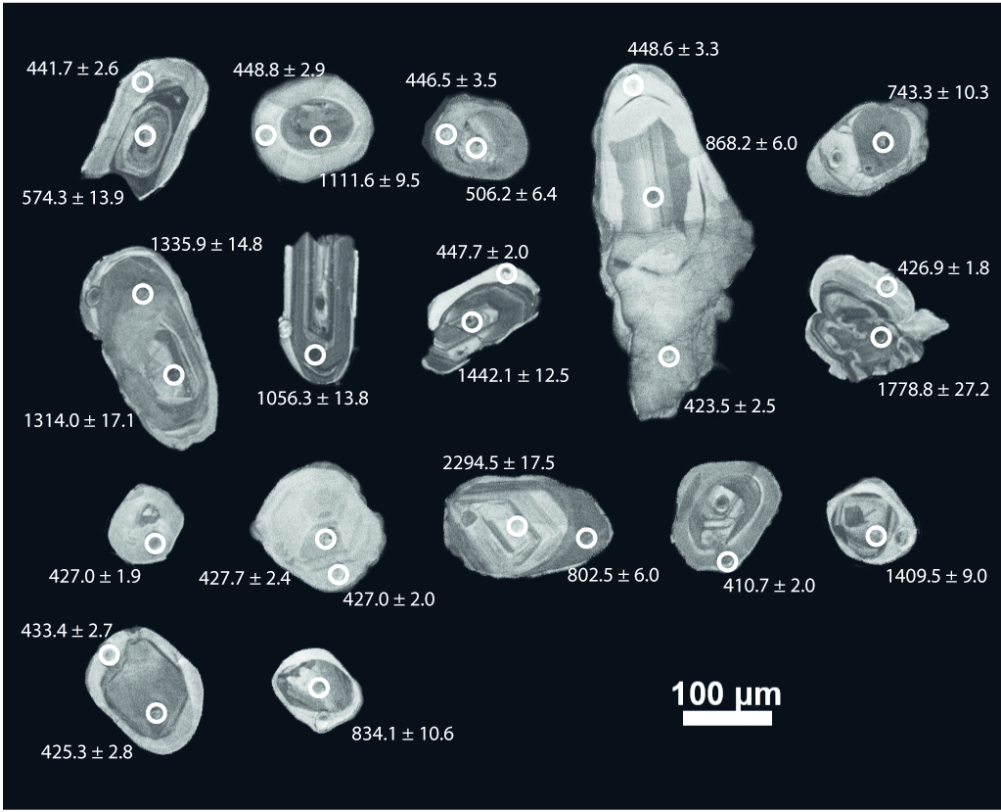


Figure 3. (Colour online) Cathodoluminescence images of representative zircon crystals from the Fjørtoft diamond-bearing garnet kyanite gneiss. White circles mark analytical spots and given numbers indicate ^{206}Pb - ^{238}U dates.

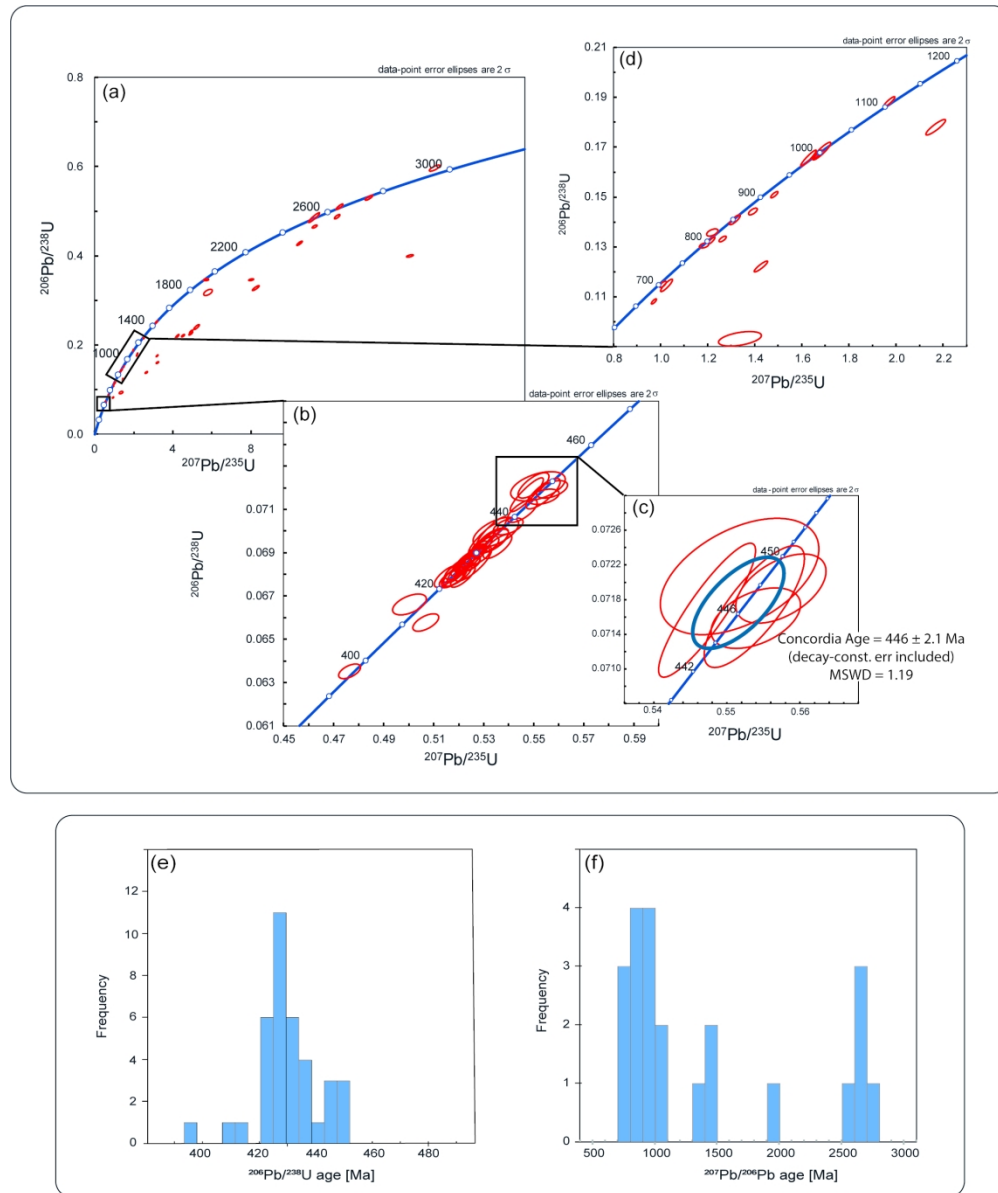


Figure 4. (Colour online) (a-d) U-Pb concordia diagram for zircon analyses; (a) all analyses for both metamorphic and detrital zircon domains, (b) concordia diagram of zircon with Caledonian ages with inset (c) showing ages for which Concordia age has been calculated. (d) Magnification of the fragment of Concordia diagram (a) showing late Precambrian dates. (e) Histogram of ^{206}Pb - ^{238}U age frequency of metamorphic zircon domains. (f) Histogram of ^{207}Pb - ^{206}Pb age frequency of concordant detrital zircon (10% discordance accepted).